Intrinsically disordered caldesmon binds calmodulin via the “buttons on a string” mechanism

Sergei E Permyakov, Eugene A Permyakov, Vladimir N Uversky

We show here that chicken gizzard caldesmon (CaD) and its C-terminal domain (residues 636-771, CaD_{136}) are intrinsically disordered proteins. The computational and experimental analyses of the wild type CaD_{136} and series of its single tryptophan mutants (W674A, W707A, and W737A) and a double tryptophan mutant (W674A/W707A) suggested that although the interaction of CaD_{136} with calmodulin (CaM) can be driven by the non-specific electrostatic attraction between these oppositely charged molecules, the specificity of CaD_{136}-CaM binding is likely to be determined by the specific packing of important CaD_{136} tryptophan residues at the CaD_{136}-CaM interface. It is suggested that this interaction can be described as the “buttons on a charged string” model, where the electrostatic attraction between the intrinsically disordered CaD_{136} and the CaM is solidified in a “snapping buttons” manner by specific packing of the CaD_{136} “pliable buttons” (which are the short segments of fluctuating local structure condensed around the tryptophan residues) at the CaD_{136}-CaM interface. Our data also show that all three “buttons” are important for binding, since mutation of any of the tryptophans affects CaD_{136}-CaM binding and since CaD_{136} remains CaM-buttoned even when two of the three tryptophans are mutated to alanines.

Intrinsically disordered caldesmon binds calmodulin via the "buttons on a string" mechanism

Sergei E. Permyakov, [†] *Eugene A. Permyakov,* [†] *and Vladimir N. Uversky*[†,‡,*]

[†]Institute for Biological Instrumentation, Russian Academy of Sciences, 142290 Pushchino, Moscow Region, Russia;

[‡]Department of Molecular Medicine and USF Health Byrd Alzheimer's Research Institute, Morsani College of Medicine, University of South Florida, Tampa, Florida 33612, USA;

*To whom correspondence should be addressed: Vladimir N. Uversky, Department of Molecular Medicine, College of Medicine, University of South Florida, 12901 Bruce B. Downs Blvd, MDC3540, Tampa, FL 33612, USA; E-mail: vuversky@health.usf.edu

ABSTRACT We show here that chicken gizzard caldesmon (CaD) and its C-terminal domain (residues 636-771, CaD_{136}) are intrinsically disordered proteins. The computational and experimental analyses of the wild type CaD_{136} and series of its single tryptophan mutants (W674A, W707A, and W737A) and a double tryptophan mutant (W674A/W707A) suggested that although the interaction of CaD_{136} with calmodulin (CaM) can be driven by the non-specific electrostatic attraction between these oppositely charged molecules, the specificity of CaD_{136}-CaM binding is likely to be determined by the specific packing of important CaD_{136} tryptophan residues at the CaD_{136}-CaM interface. It is suggested that this interaction can be described as the "buttons on a charged string" model, where the electrostatic attraction between the intrinsically disordered CaD_{136} and the CaM is solidified in a "snapping buttons" manner by specific packing of the CaD_{136} "pliable buttons" (which are the short segments of fluctuating local structure condensed around the tryptophan residues) at the CaD_{136}-CaM interface. Our data also show that all three "buttons" are important for binding, since mutation of any of the tryptophans affects CaD_{136}-CaM binding and since CaD_{136} remains CaM-buttoned even when two of the three tryptophans are mutated to alanines.

ABBREVIATIONS

AIBS, disorder-based ANCHOR-identified binding site; CaD, caldesmon; CaD_{136}, C-terminal domain (636-771) of CaD; CaM, calmodulin; CD, circular dichroism; DSC, differential scanning calorimetry; IDP, intrinsically disordered protein; IDPR, intrinsically disordered protein region; MoRF, molecular recognition feature; PTM, posttranslational modification; UV, ultra violet

INTRODUCTION

Caldesmon, CaD, is a ubiquitous actin-binding protein of ~770 residues with the molecular mass of 88.75 kDa and *pI* of 5.56 (Mabuchi et al. 1996). CaD is involved in the regulation of smooth muscle contraction, non-muscle motility, and cytoskeleton formation (Czurylo & Kulikova 2012; Gusev 2001; Marston & Redwood 1991; Martson & Huber 1996; Matsumura & Yamashiro 1993; Sobue & Sellers 1991). Particularly, CaD plays a role in a thin-filament-linked regulation of smooth muscle contraction through specific binding to F-actin and F-actin-tropomyosin leading to the inhibition of the actin-stimulated myosin ATPase (Marston & Redwood 1991). The inhibitory action of CaD is reversed by interaction of this protein with various calcium-dependent proteins, such as calmodulin (CaM), caltropin (Mani & Kay 1996), S100 proteins (Polyakov et al. 1998) and calcyclin (Kuznicki & Filipek 1987). The functional activity of CaD is further regulated by phosphorylation at multiple sites (Shirinsky et al. 1999). CaD is also engaged in the interaction with F-actin (Adelstein & Eisenberg 1980; Gusev 2001). These thin filament-based modulatory effects provide additional "fine-tuning" to the well-established, myosin light chain phosphorylation-dependent, thick filament-based regulation of smooth muscle contraction (Adelstein & Eisenberg 1980). CaD is found to form tight complexes with several proteins, such as myosin, actin, CaM (Marston & Redwood 1991), caltropin (Gusev 2001; Mani & Kay 1996), calcyclin (Kuznicki & Filipek 1987), $S100a_o$, S100a and S100b proteins (Polyakov et al. 1998), and non-muscle tropomyosin (Gusev 2001). It also possesses distinctive phospholipid-binding properties (Czurylo et al. 1993; Makowski et al. 1997; Vorotnikov et al. 1992; Vorotnikov & Gusev 1990).

Sequence of CaD can be divided to four independent functional domains. The first N-terminal domain interacts with myosin and tropomyosin. The second domain is characteristic for smooth

59 muscle CaD and also participates in the tropomyosin binding. The third domain is involved in
60 the CaD interaction of with myosin, tropomyosin, and actin. The fourth C-terminal domain plays
61 the most important role in the function of CaD, interacting with actin, various Ca^{2+}-binding
62 proteins, myosin, tropomyosin, and phospholipids (Gusev 2001). Furthermore, interaction of
63 CaD with actin, tropomyosin, and CaM involves multiple sites (Fraser et al. 1997; Gusev 2001;
64 Huber et al. 1996; Medvedeva et al. 1997; Wang et al. 1997), with CaD being wrapped around
65 its partners (Gusev 2001; Permyakov et al. 2003).

66 CaD exists as two isoforms that are generated by alternative splicing of a single mRNA
67 transcript. These CaD isoforms are differently distributed among tissues (Abrams et al. 2012;
68 Kordowska et al. 2006). The light (or low molecular weight) isoform (l-CaD) is expressed in
69 most cell types, including at low levels in smooth muscle, where it mediates actin and non-
70 muscle myosin interaction in the cortical cytoskeleton (Helfman et al. 1999). The heavy (or high
71 molecular weight) isoform (h-CaD) is expressed specifically in smooth muscle. It is believed that
72 this isoform is capable of simultaneous binding to smooth muscle actin and myosin filaments due
73 to the presence of a peptide spacer domain in the middle of the protein (Wang et al. 1991).

74 Based on these functional peculiarities (the ability to interact with multiple binding partners,
75 the presence of numerous sites of posttranslational modifications, the capability to be engaged in
76 wrapping interactions, and the presence of multiple alternatively spliced isoforms) one could
77 conclude that CaD belongs to the realm of the intrinsically disordered proteins (IDPs), which
78 were recognized quite recently (Dunker et al. 2001; Dunker et al. 2008a; Dunker et al. 2008b;
79 Dyson & Wright 2005; Tompa 2002; Uversky 2002a; Uversky 2002b; Uversky 2010; Uversky &
80 Dunker 2010; Uversky et al. 2000; Wright & Dyson 1999) as important biologically active
81 proteins without unique 3D-structures that represent a crucial extension of the protein kingdom

(Dunker et al. 2008a; Dyson 2011; Tompa 2012; Turoverov et al. 2010; Uversky 2002a; Uversky 2003; Uversky 2013a; Wright & Dyson 1999). IDPs and hybrid proteins containing both ordered and intrinsically disordered domains/regions (Dunker et al. 2013) are very common in nature (Dunker et al. 2000; Tokuriki et al. 2009; Uversky 2010; Ward et al. 2004; Xue et al. 2012a; Xue et al. 2010b). They constitute significant fractions of all known proteomes, where the overall amount of disorder in proteins increases from bacteria to archaea to eukaryota, and over a half of the eukaryotic proteins are predicted to possess long IDP regions (IDPRs) (Dunker et al. 2000; Oldfield et al. 2005a; Uversky 2010; Ward et al. 2004; Xue et al. 2012b). Due to the lack of unique 3D-structures, IDPs/IDPRs carry out numerous crucial biological functions (such as signaling, regulation, and recognition) (Daughdrill et al. 2005; Dunker et al. 2002a; Dunker et al. 2002b; Dunker et al. 2005; Dunker et al. 1998; Dunker et al. 2001; Dyson & Wright 2005; Tompa 2002; Tompa 2005; Tompa & Csermely 2004; Tompa et al. 2005; Uversky 2002a; Uversky 2002b; Uversky 2003; Uversky 2010; Uversky et al. 2000; Uversky et al. 2005; Vucetic et al. 2007; Wright & Dyson 1999; Xie et al. 2007a; Xie et al. 2007b) that complement functions of ordered proteins.(Vucetic et al. 2007; Xie et al. 2007a; Xie et al. 2007b) Furthermore, many IDPs/IDPRs are associated with the variety of human diseases (Uversky et al. 2014; Uversky et al. 2008).

In our previous study, we showed that the C-terminal domain of chicken gizzard CaD, CaD_{136} (636-771 fragment), is a typical extended IDP characterized by the almost complete lack of secondary structure, absence of a globular core, and a large hydrodynamic volume (Permyakov et al. 2003). Although CaD_{136} can effectively bind to the Ca^{2+}-loaded CaM, this protein was shown to remain mostly unfolded within its complex with CaM (Permyakov et al. 2003). In this paper, we first performed comprehensive computational characterization of chicken gizzard CaD

105 to confirm the overall disorder status of this protein. Then, we found that the CaD_{136} has three
106 major disorder-based potential binding sites located around the tryptophan residues W674,
107 W707, and W737. To verify the role of these sites in CaD_{136} binding to CaM, we designed and
108 characterized biophysically three single tryptophan mutants (W674A, W707A, and W737A) and
109 a double tryptophan mutant (W674A/W707A). This analysis suggests that CaD_{136} potentially
110 binds CaM via the "buttons on a charged string" mechanism. Some biological significance of
111 these observations is discussed.

112

113 **MATERIALS AND METHODS**

114 **Materials**

115 Samples of chicken gizzard CaM, CaD_{136}, its single tryptophan mutants (W674A, W707A, and
116 W737A), and a double tryptophan mutant (W674A/W707A) were a kind gift of Dr. Yuji
117 Kobajashi (Department of Physical Chemistry, Institute of Protein Research, Osaka University,
118 Osaka 565, Japan).

119 All chemicals were of analytical grade from Fisher Chemicals. Concentrations of CaD and
120 CaM were estimated spectrophotometrically. Molar extinction coefficient for CaM was
121 calculated based upon amino acids content according to (Pace et al. 1995): ε_{280nm}=2,980 $M^{-1}cm^{-1}$.
122 For the wild type CaD ε_{280nm}=17,990 $M^{-1}cm^{-1}$ was used, whereas molar extinction coefficients
123 for single and double tryptophan mutants were taken to be ε_{280nm}=12,490 $M^{-1}cm^{-1}$ and
124 ε_{280nm}=6,990 $M^{-1}cm^{-1}$, respectively.

125

126 **Methods**

Absorption Spectroscopy. Absorption spectra were measured on a spectrophotometer designed and manufactured in the Institute for Biological Instrumentation (Pushchino, Russia).

Circular Dichroism Measurements. Circular dichroism measurements were carried out by means of a AVIV 60DS spectropolarimeter (Lakewood, N. J., USA), using cells with a path length of 0.1 and 10.0 mm for far and near UV CD measurements, respectively. Protein concentration was kept at 0.6-0.8 mg/ml throughout all the experiments.

Fluorescence Measurements. Fluorescence measurements were carried out on a lab-made spectrofluorimeter main characteristics of which were described earlier (Permyakov et al. 1977). All spectra were corrected for spectral sensitivity of the instrument and fitted to log-normal curves (Burstein & Emelyanenko 1996) using nonlinear regression analysis (Marquardt 1963). The maximum positions of the spectra were obtained from the fits. The temperature inside the cell was monitored with a copper-constantan thermopile.

Parameters of CaD136 Binding to CaM. The apparent binding constants for complexes of calmodulin with the caldesmon mutants were evaluated from a fit of the fluorescence titration data to the specific binding scheme using nonlinear regression analysis (Marquardt 1963). The binding scheme was chosen on the “simplest best fit” basis. The quality of the fit was judged by a randomness of distribution of residuals. Temperature dependence of intrinsic fluorescence was analyzed according to (Permyakov & Burstein 1984).

149 *Differential Scanning Microcalorimetry.* Scanning microcalorimetric measurements were
150 carried out on a DASM-4M differential scanning microcalorimeter (Institute for Biological
151 Instrumentation of the Russian Academy of Sciences, Pushchino, Russia) in 0.48 mL cells at a 1
152 K/min heating rate. An extra pressure of 1.5 atm was maintained in order to prevent possible
153 degassing of the solutions on heating. Protein concentrations were in the 0.5 to 0.7 mg/mL range.
154 The heat sorption curves were baseline corrected by heating the measurement cells filled by the
155 solvent only. Specific heat capacities of the proteins were calculated according to (Privalov
156 1979; Privalov & Potekhin 1986).

157

158 *Sequence Analyses.* Amino acid sequences of human and chicken caldesmons (UniProt IDs:
159 P12957 and Q05682, respectively) and human and chicken calmodulins (UniProt IDs: P62149
160 and P62158, respectively) were retrieved from UniProt (http://www.uniprot.org/).

161 The intrinsic disorder propensities of query proteins were evaluated by several per-residues
162 disorder predictors, such as PONDR® VLXT (Dunker et al. 2001), PONDR® VSL2 (Peng et al.
163 2005), PONDR® VL3 (Peng et al. 2006b), and PONDR® FIT (Xue et al. 2010a). Here, scores
164 above 0.5 are considered to correspond to the disordered residues/regions. PONDR® VSL2B is
165 one of the more accurate stand-alone disorder predictors (Fan & Kurgan 2014; Peng et al. 2005;
166 Peng & Kurgan 2012), PONDR® VLXT is known to have high sensitivity to local sequence
167 peculiarities and can be used for identifying disorder-based interaction sites (Dunker et al. 2001),
168 whereas a metapredictor PONDR-FIT is moderately more accurate than each of the component
169 predictors, PONDR® VLXT (Dunker et al. 2001), PONDR® VSL2 (Peng et al. 2005), PONDR®
170 VL3 (Peng et al. 2006b), FoldIndex (Prilusky et al. 2005), IUPred (Dosztanyi et al. 2005a), and

171 TopIDP (Campen et al. 2008). Disorder propensities of CaD and CaM were further analyzed
172 using the MobiDB database (http://mobidb.bio.unipd.it/) (Di Domenico et al. 2012; Potenza et al.
173 2015) that generates consensus disorder scores based on the outputs of ten disorder predictors,
174 such as ESpritz in its two flavors (Walsh et al. 2012), IUPred in its two flavors (Dosztanyi et al.
175 2005a), DisEMBL in two of its flavors (Linding et al. 2003a), GlobPlot (Linding et al.
176 2003b), PONDR® VSL2B (Obradovic et al. 2005; Peng et al. 2006a), and JRONN (Yang et al.
177 2005).

178 For human CaM and CaD proteins, disorder evaluations together with the important disorder-
179 related functional annotations were retrieved from D^2P^2 database (http://d2p2.pro/) (Oates et al.
180 2013). D^2P^2 is a database of predicted disorder that represents a community resource for pre-
181 computed disorder predictions on a large library of proteins from completely sequenced genomes
182 (Oates et al. 2013). D^2P^2 database uses outputs of PONDR® VLXT (Dunker et al. 2001), IUPred
183 (Dosztanyi et al. 2005a), PONDR® VSL2B (Obradovic et al. 2005; Peng et al. 2006a), PrDOS
184 (Ishida & Kinoshita 2007), ESpritz (Walsh et al. 2012), and PV2 (Oates et al. 2013). This
185 database is further enhanced by information on the curated sites of various posttranslational
186 modifications and on the location of predicted disorder-based potential binding sites.

187 Interactability of chicken CaD and CaM was evaluated by STRING (Search Tool for the
188 Retrieval of Interacting Genes, http://string-db.org/), which is the online database resource, that
189 provides both experimental and predicted interaction information (Szklarczyk et al. 2011).
190 STRING produces the network of predicted associations for a particular group of proteins. The
191 network nodes are proteins, whereas the edges represent the predicted or known functional
192 associations. An edge may be drawn with up to 7 differently colored lines that represent the
193 existence of the seven types of evidence used in predicting the associations. A red line indicates

194 the presence of fusion evidence; a green line - neighborhood evidence; a blue line – co-
195 occurrence evidence; a purple line - experimental evidence; a yellow line – text mining evidence;
196 a light blue line - database evidence; a black line – co-expression evidence (Szklarczyk et al.
197 2011).

198 Potential disorder-based binding sites in CaD_{136} (which is the C-terminal domain (636-771) of
199 CaD) were found using three computational tools, α-MoRF identifier (Cheng et al. 2007;
200 Oldfield et al. 2005b), ANCHOR (Dosztanyi et al. 2009; Meszaros et al. 2009), and MoRFpred
201 (Disfani et al. 2012). Since IDPs/IDPRs are commonly involved in protein-protein interactions
202 (Daughdrill et al. 2005; Dunker et al. 2002a; Dunker et al. 2002b; Dunker et al. 2001; Dunker et
203 al. 2008b; Dunker & Uversky 2008; Oldfield et al. 2005b; Radivojac et al. 2007; Tompa 2002;
204 Uversky 2011b; Uversky 2012; Uversky 2013b; Uversky & Dunker 2010; Uversky et al. 2005),
205 and since they are able to undergo at least partial disorder-to-order transitions upon binding,
206 which is crucial for recognition, regulation, and signaling (Dunker et al. 2001; Dyson & Wright
207 2002; Dyson & Wright 2005; Mohan et al. 2006; Oldfield et al. 2005b; Uversky 2013b; Uversky
208 2013c; Uversky et al. 2000; Vacic et al. 2007a; Wright & Dyson 1999), these proteins and
209 regions often contain functionally important, short, order-prone motifs within the long disordered
210 regions. Such motifs are known as Molecular Recognition Feature (MoRF), they are able to
211 undergo disorder-to-order transition during the binding to a specific partner, and can be
212 identified computationally (Cheng et al. 2007; Oldfield et al. 2005b). For example, an α-MoRF
213 predictor indicates the presence of a relatively short, loosely structured region within a largely
214 disordered sequence (Oldfield et al. 2005b), which can gain functionality upon a disorder-to-
215 order transition induced by binding to partners (Mohan et al. 2006; Vacic et al. 2007a). In
216 addition to MoRF identifiers, potential binding sites in disordered regions can be identified by

the ANCHOR algorithm (Dosztanyi et al. 2009; Meszaros et al. 2009). This approach relies on the pairwise energy estimation approach developed for the general disorder prediction method IUPred (Dosztanyi et al. 2005a; Dosztanyi et al. 2005b). being based on the hypothesis that long regions of disorder contain localized potential binding sites that cannot form enough favorable intrachain interactions to fold on their own, but are likely to gain stabilizing energy by interacting with a globular protein partner (Dosztanyi et al. 2009; Meszaros et al. 2009). Regions of a protein suggested by the ANCHOR algorithm to have significant potential to be binding sites are the ANCHOR-indicated binding site (AIBS).

RESULTS AND DISCUSSION

Characterization of Functional Disorder in Caldesmon and Calmodulin

The amino acid sequences and compositions of IDPs/IDPRs are significantly different from those of ordered proteins and domains. For example, the amino acid compositions of extended IDPs/IDPRs (i.e., highly disordered proteins and regions lacking almost any residual structure (Dunker et al. 2001; Uversky 2002a; Uversky 2002b; Uversky 2003; Uversky 2013a; Uversky 2013c; Uversky & Dunker 2010; Uversky et al. 2000)) are characterized by high mean net charge and low mean hydropathy, being significantly depleted in order-promoting residues C, W, Y, F, H, I, L, V, and N and significantly enriched in disorder-promoting residues A, R, G, Q, S, P, E, and K (Dunker et al. 2001; Radivojac et al. 2007; Romero et al. 2001; Vacic et al. 2007b). The fractional difference in composition between CaD and a set of ordered proteins from PDB Select 25 (Berman et al. 2000) was calculated as $(C_{CaD}-C_{order})/C_{order}$, where C_{CaD} is the content of a given amino acid in CaD, and C_{order} is the corresponding value for the set of ordered proteins. This analysis revealed that in comparison with typical ordered proteins, CaD is significantly

depleted in major order-promoting residues (C, Y, F, H, V, L, and I) and is significantly enriched in major disorder-promoting residues, such as A, R, E, and K. This means that CaD might contain multiple structural and functional signatures typical for the IDPs.

In agreement with this conclusion, Figure 1A represents the results of the disorder predisposition analysis in CaD by a family of PONDR disorder predictors, PONDR® VLXT (Dunker et al. 2001), PONDR® VSL2 (Peng et al. 2005), PONDR® VL3 (Peng et al. 2006b), and PONDR® FIT (Xue et al. 2010a). Since the absolute majority of residues is predicted to have disorder scores above 0.5 and since the mean disorder score for the full-length protein ranges, depending on the predictor, from 0.69 to 0.93, this analysis clearly shows that CaD is expected to be mostly disordered. In agreement with this conclusion, the consensus MobiDB analysis (http://mobidb.bio.unipd.it/entries/P12957) revealed that chicken gizzard CaD contains 98.4% disordered residues. Curiously, the C-terminal domain of this protein, CaD_{136}, is predicted to be a bit more predisposed for order than the remaining protein (depending on the predictor, the mean disorder score for this 636-771 fragment of CaD ranges from 0.52 to 0.81). This observation is further illustrated by Figure 1B which represents the PONDR-based disorder profiles of this region.

Curiously, although several X-ray crystal (PDB IDs: 1ahr, 1up5, 2bcx, 2bki, 2o5g, 2o60, 2vb6, 3gog, and 3gp2) and NMR solution structures (PDB IDs: 2kz2 and 2m3s) of CaM are known, Figure 1C shows that this protein is predicted to be rather disordered too. These findings are not too surprising, since it is known that the CaM structure and folding are strongly dependent on the metal ion binding (Li et al. 2014; Sulmann et al. 2014), and that there is a great variability in the crystal structures of CaM in isolation (i.e., where it is not bound to its protein or peptide partners and exists in the unliganded form) which is considered as an illustration of CaM plasticity in

solution (Kursula 2014). Furthermore, several studies on the structure of unliganded CaM in solution using small angle scattering and other methods have indicated the presence of a mixture of conformations (Bertini et al. 2010; Heller 2005; Kursula 2014; Yamada et al. 2012). Also in agreement with these predictions, the analysis of one of the NMR structures of CaM (PDB ID: 2m3s) revealed that this protein might contain up to 50.3% of disordered residues in solution (Moroz et al. 2013). Again, the results of the per-residue predictions by the members of the PONDR family are further supported by the results of the MobiDB analysis, according to which the consensus disorder content of CaM based on the outputs of ten disorder predictors is 18.1%. The corresponding values evaluated by the individual predictors (http://mobidb.bio.unipd.it/entries/P62149) are ranging from 6.0% and 13.4% for the ESpritz-XRay and DisEMBL-465, respectively to 41.6% and 69.1% for the IUPred-long and PONDR® VSL2, respectively. Note that both ESpritz-XRay and DisEMBL-465 are trained based on proteins with known crystal structures and containing regions of missing electron density, whereas IUPred-long and PONDR VSL2 use different criteria for training.

Further information on the functional disorder status of CaD and CaM was retrieved from D^2P^2 portal, which represents a database of pre-computed disorder predictions for a large library of proteins from completely sequenced genomes (Oates et al. 2013), which in addition to outputs of nine disorder predictors provides information on the curated sites of various posttranslational modifications and on the location of predicted disorder-based potential binding sites. Since this database does not include data for chicken, the human homologues of CaD and CaM were used for this analysis. The validity of this approach is justified by the fact that sequences of human and chicken CaMs are identical (100% identity), whereas sequences of human and chicken CaD are highly conserved (61% identity).

286 Figures 2A and 3A represents the results of this analysis of CaD and CaM, respectively, and
287 provide further support for the abundance and functional importance of intrinsic disorder in these
288 proteins, which are predicted to contain long disordered regions enriched in potential disorder-
289 based binding motifs and containing numerous predicted sites of potential posttranslational
290 modifications (PTMs). The fact that disordered domains/regions of the human CaD and CaM
291 contain numerous PTM sites is in agreement with the well-known notion that
292 phosphorylation(Iakoucheva et al. 2004) and many other enzymatically catalyzed PTMs are
293 preferentially located within the IDPRs (Pejaver et al. 2014).
294 The interactivity of chicken CaD and CaM was evaluated by the online database resource,
295 STRING, which provides information on both experimental and predicted interactions
296 (Szklarczyk et al. 2011). Figure 2B and 3B clearly show that both proteins are predicted to have
297 numerous binding partners. Predicted here high levels of connectivity and binding promiscuity
298 indicate that, in the related protein-protein interaction networks (PPI), chicken CaD and CaM
299 serve as hub proteins connecting biological modules to each other. The binding promiscuity of
300 hub proteins is believed to be dependent on intrinsic disorder (Dosztanyi et al. 2006; Ekman et
301 al. 2006; Haynes et al. 2006; Patil & Nakamura 2006; Singh et al. 2006; Uversky et al. 2005),
302 where disorder and related disorder-to-order transitions enable one protein to interact with
303 multiple partners (one-to-many signaling) or enable multiple partners to bind to one protein
304 (many-to-one signaling) (Dunker et al. 1998). In line with these considerations, intrinsically
305 disordered nature of chicken CaD and CaM provides a plausible explanation for their potential
306 roles as hub proteins. Therefore, data reported in Figures 1, 2 and 3 suggest that both CaD and
307 CaM are expected to contain substantial amounts of functional disorder, which CaD being
308 predicted to be mostly disordered.

309 Figure 1D shows that the positively charged R and K residues are evenly distributed within the
310 CaD_{136} sequence and that the sequence of CaM contains evenly spread negatively charged
311 residues D and E. Since under the physiologic conditions of neutral pH, the C-terminal
312 interacting domain of CaD and CaM possess charges of opposite sign (+9 for CaD_{136} and -24 for
313 CaM) it is likely that electrostatic interactions play important role in interaction between these
314 two proteins. This hypothesis is further supported by Figure 4, which represents the charge
315 distribution over the CaM surface and shows that negative charges are almost evenly distributed
316 over the entire protein surface. What then defines the specificity of interaction between a highly
317 positively charged IDP (CaD_{136}) and a highly negatively charged surface of CaM? Some answers
318 to this important question can be obtained analyzing peculiarities of the disorder distribution in
319 CaD_{136}. In fact, many IDPs/IDPRs involved in protein-protein interactions and molecular
320 recognitions are able to undergo at least partial disorder-to-order transitions upon binding
321 (Daughdrill et al. 2005; Dunker et al. 2002a; Dunker et al. 2002b; Dunker et al. 2001; Dunker et
322 al. 2008b; Dunker & Uversky 2008; Dyson & Wright 2002; Dyson & Wright 2005; Mohan et al.
323 2006; Oldfield et al. 2005b; Radivojac et al. 2007; Tompa 2002; Uversky 2011b; Uversky 2012;
324 Uversky 2013b; Uversky 2013c; Uversky & Dunker 2010; Uversky et al. 2000; Uversky et al.
325 2005; Vacic et al. 2007a; Wright & Dyson 1999). Such potential disorder-based binding sites are
326 known as Molecular Recognition Feature (MoRF), and they often can be found based on the
327 peculiar shape of a disorder profile (sharp "dips" within the long IDPRs). These observations
328 serve as a foundation for the corresponding computational tools, e.g., α-MoRF-Pred (Cheng et al.
329 2007; Oldfield et al. 2005b) or MoRFpred (Disfani et al. 2012). Alternatively, the disorder-based
330 binding sites can be identified by ANCHOR (Dosztanyi et al. 2009; Meszaros et al. 2009) (see

Materials and Methods). There is generally a good agreement between the results of binding sites prediction by these two tools.

These analyses revealed that CaD_{136} has several disorder-based potential binding sites and three of them correspond to the major minima in the CaD_{136} disorder plots obtained by both PONDR® VLXT and PONDR-FIT (see Figure 5). Since each of these three dip-centered potential binding sites include a tryptophan residue, we decided to mutate those tryptophans in order to evaluate their roles in the CaD_{136} binding to CaM. At the first stage, the disorder propensities of three single tryptophan mutants (W674A, W707A, and W737A) and a double tryptophan mutant (W674A/W707A) were compared using PONDR® VLXT and PONDR FIT algorithms. Figure 5 represents the results of these analyses and shows that the local disorder propensities were noticeably affected by single mutations W674A and W707A and by the W674A/W707A double mutation, whereas W737A had a very minimal effect on the CaD_{136} disorder profile. Although the depth of corresponding disorder minima was affected by mutations, none of these tryptophan-to-alanine substitutions completely eliminated dips. These data suggested that binding affinity of CaD_{136} can be moderately affected by single substitutions W674A and W707A, and that the W674A/W707A double mutation could have somewhat stronger effect on protein-protein interactions. To check these predictions, we analyzed biophysical properties and binding affinities of three single tryptophan mutants W674A, W707A, and W737A, and a double tryptophan mutant W674A/W707A. Results of these analyses are represented below.

352 **Effect of tryptophan substitutions on tryptophan fluorescence spectrum of the C-terminal**
353 **CaD domain**

354 Analysis of the normalized tryptophan fluorescence spectra of CD_{136} and its mutants in
355 solution and in complex with CaM (which does not have tryptophan residues) revealed that the
356 spectra of all the CD_{136} proteins in their unbound forms are practically the same (see Figure S1).
357 They have extremely long wavelength positions and are similar to spectrum of a free tryptophan
358 in water, which shows that in all these proteins, the tryptophan residues are totally exposed to
359 water. The spectra of the complexes with CaM are different. The CaM-complexes W737A
360 mutant has the most blue-shifted spectrum, whereas the W707A mutant in its bound state has the
361 least blue-shifted spectrum. The Table 1 represents the relative fluorescence quantum yields for
362 CD_{136} and its mutants in solution and in the complex with CaM.
363

364 **Effect of tryptophan substitutions on far-UV CD spectra of CaD_{136} mutants**

365 Figure 6 represents the far-UV CD spectra of wild type, W674A, W707A, W737A and
366 W674A/W707A CaD_{136} and shows that all these proteins have far-UV CD spectra typical of the
367 almost completely unfolded polypeptides. In other words, the data are consistent with the
368 conclusion that at physiological conditions none of the CaD_{136} domains has considerable amount
369 of ordered secondary structure; i.e., they belong to the family of so-called natively unfolded
370 proteins, which are the most disordered members of the realm of intrinsically disordered
371 proteins. On the other hand, more detailed analysis of the far-UV CD spectrum shows that the
372 wild type CaD_{136}, being mostly disordered, is still far from to be completely unfolded and
373 preserves some residual structure (e.g., $[\theta]_{222} \sim -3{,}000$ deg cm^2 dmol^{-1}, the minimum is located at
374 200, rather than at 196-198 nm, see Figure 6).

375 Figure 6 shows that all amino acid substitutions affect the far-UV CD spectrum of the C-
376 terminal CaD domain in a similar manner, inducing considerable decrease in the spectrum
377 intensity around 200 nm. This is further illustrated by Figure S2 that represents the difference
378 spectra between the wild type CaD_{136} and mutated domains and clearly shows that all the amino
379 acid substitutions induce noticeable additional unfolding of the residual structure in the originally
380 rather disordered protein.
381
382 **Effect of tryptophan substitutions on the near-UV CD spectra of CaD_{136} mutants**
383 Surprisingly, Figure 7 shows that wild type CaD_{136} and all its mutants possess rather intensive
384 and pronounced near-UV CD spectra. This means that tryptophan residues of these proteins are
385 in relatively asymmetric environment. Figure 7 shows that any tryptophan substitution analyzed
386 in this study has a considerable effect on the near-UV CD spectrum of CaD_{136}, leading to the
387 substantial decrease in the spectral intensity. It also can be seen that different tryptophan residues
388 have different contributions to the near-UV CD spectrum of protein. In fact, Figure 7 shows that
389 the effect of amino acid substitutions increases in the following order: W707A < W737A <
390 W674A ≤ W674A/W707A. This conclusion is confirmed by the difference spectra shown in
391 Figure S3. Therefore, these data suggest that tryptophan residues have noticeable contributions to
392 the residual structure of CaD_{136}, likely serving as condensation centers around which the local
393 dynamic structure is formed.
394

Conformational stability of CaD_{136} and its mutants analyzed by the effect of temperature on their near- and far-UV CD spectra

Figure 8 represents near-UV CD spectra of the wild type and mutated CaD_{136} measured at different temperatures. It can be seen that heating affects the near-UV CD spectra of different proteins in different manner. In the case of the wild type protein, some initial decrease in the spectral intensity at 40°C is followed by the increase in spectral intensity at higher temperatures. Interestingly, after the cooling, the near-UV CD spectrum of this variant is somewhat more intensive than spectrum measured before the heating. Spectrum of W674A mutant increases with the temperature and this effect is reversible. Mutants W707A and W737A show reversible decrease in spectral intensity, whereas spectrum of the double W674A/W707A mutant is practically unaffected by temperature. Importantly, Figure 8 shows that even at 90°C all of the protein variants analyzed in this study show pronounced near-UV CD spectra, reflecting the fact that the temperature increase does not destroy completely the asymmetric environment of their aromatic residues.

Temperature had similar effect of the far-UV CD spectra of all the CaD_{136} variants. As an example, Figure 9A represents the far-UV CD spectra of W674A mutant measured at different temperatures. It can be seen that shape and intensity of the spectrum undergo considerable changes with the increase in temperature, reflecting the temperature-induced formation of the more ordered secondary structure. Same spectral changes were observed for several other IDPs and were classified as the “turn-out” paradoxical response of extended IDPs (opposite to the response of ordered proteins) to changes in their environment (Uversky 2002a; Uversky 2002b; Uversky 2011a; Uversky 2013a; Uversky 2013c; Uversky & Dunker 2010). Figure 9B summarizes the data on the effect of heating on the secondary structure of the CaD_{136} variants as

corresponding $[\theta]_{222}$ *vs*. temperature dependences. One can see that in all cases studied temperature increase was accompanied by the steady increase in the negative ellipticity at 222 nm. It is necessary to emphasize here that this behavior is totally different from the conformational behavior of typical globular proteins, which show temperature-induced reduction in the content of ordered secondary structure.

Studying the CaD_{136} variants by scanning microcalorimetry

Figure S4 represents the calorimetric scans obtained for the wild type CaD_{136} and its mutants. The absolute values of the specific heat capacity (ranging from ~2 to 3 J/(g·K)) and the absence of distinct heat absorption peaks within the temperature region from 10 to 100ºC for these proteins suggest that their structure is predominantly unfolded.

Interactions of the CaD_{136} and its tryptophan mutants with calmodulin studied by intrinsic fluorescence

Figure 10 represents the results of the spectrofluorimetric titration of CD_{136} and its tryptophan mutants with CaM. The increase in CaM concentration induces an increase in fluorescence quantum yield and a blue shift of the fluorescence spectrum maximum (see also data presented in Figure S1 and Table 1). The points shown in this figure are experimental data, and the curves are theoretical fits. The corresponding curves were computed using the simplest one-site binding scheme by fitting the experimental points varying the binding constant. The values of the binding constants which give the best fits are collected in the Table 1. This analysis revealed that the substitution of the tryptophan residues by alanines resulted in a decrease in the CaD_{136}-CaM binding constant in all the cases except W737A, where mutation caused an increase

441 in the CaD_{136} affinity for CaM. Table 1 also shows that the double W674A/W707A mutation
442 caused the largest reduction in the CaD_{136} binding efficiency. The value of the association
443 constant for wild type CaD_{136} in our work is in a good agreement with the literature data of
444 another authors (Czurylo et al. 1991; Graether et al. 1997; Huber et al. 1996; Medvedeva et al.
445 1997; Shirinsky et al. 1988; Wang et al. 1997).

446 The ability of the caldesmon and its C-terminal fragments to interact specifically with
447 calmodulin has been established long ago (Shirinsky et al. 1988), and several models of this
448 complex have been suggested (reviewed in (Gusev 2001)). It is known that the C-terminal
449 domain of CaD contains three CaM-binding sites, centers A (close to Trp674), B (close to
450 Trp707), and B' (close to Trp737). It has been shown that sites A and B interact with C-terminal
451 lobe of CaM (this protein has dumbbell shape with two α-helical Ca^{2+}-binding globular domains,
452 separated by an extended "handle" formed by a seven-turn α-helix), whereas center B forms
453 complex with the N-terminal globular domain (Gusev 2001; Marston et al. 1994; Mezgueldi et
454 al. 1994; Zhan et al. 1991). The idea of multiple-sited interaction of CaD and CaM and
455 participation of Trp residues in it was described earlier in a series of papers from different
456 laboratories (for instance, (Huber et al. 1996; Mezgueldi et al. 1994). For example, to determine
457 the contribution of each of three Trp residues (659, 692, and 722, which are similar to 674, 707,
458 and 737 in our protein) in the calmodulin-caldesmon interaction, Graether *et al*. (1997) have
459 mutated the Trp residues to Ala in the C-terminal domain of fibroblast caldesmon (CaD39) and
460 studied the effects on calmodulin binding by fluorescence measurements and using immobilized
461 calmodulin (Graether et al. 1997). All the mutations reduced the affinity of CaD to calmodulin,
462 but mutation of Trp 722 at site B' to Ala caused the smallest decrease in affinity. In our work
463 similar mutation caused even an increase in affinity. The authors concluded that Trp 659 and Trp

692 are the major determinants in the fibroblast caldesmon-calmodulin interaction and that Trp 722 in site B' plays a minor role (Graether et al. 1997). The results of our study show that in gizzard caldesmon the letter tryptophan seems to play more significant role in the interaction with calmodulin.

CONCLUSIONS

Altogether, data presented in our study suggest that CaD and its C-terminal domain, CaD_{136}, are intrinsically disordered proteins. CaD potentially serves as a disordered hub in several important protein-protein interaction networks. It is likely that CaD_{136}-CaM interaction is driven by the non-specific electrostatic attraction interactions due to the opposite charges of these two proteins. Specificity of CaD_{136}-CaM binding is likely to be determined by the definite packing of important tryptophan residues at the CaD_{136}-CaM interface, which is manifested by the dramatic blue shift of the intrinsic CaD_{136} fluorescence. In its non-bound form, CaD_{136} is highly disordered, with the aforementioned tryptophan residues potentially serving as centers of local fluctuating structural elements. Therefore, our bioinformatics and experimental data suggest that the interaction between CaD_{136} and CaM can be described within the "buttons on a charged string" model, where the electrostatic attraction between the positively charged and highly disordered CaD_{136} containing at least three segments of fluctuating local structure ("pliable buttons") and the negatively charged CaM is solidified by the specific packing of three short regions containing tryptophan residues in a "snapping a button" manner. This model is schematically represented in Figure 11. Curiously, it seems that all three "buttons" are important for binding, since mutation of any of the tryptophans affects CaD_{136}-CaM binding and since CaD_{136} remains CaM-buttoned even when two of the three tryptophans are mutated to alanines.

REFERENCES

Abrams J, Davuluri G, Seiler C, and Pack M. 2012. Smooth muscle caldesmon modulates peristalsis in the wild type and non-innervated zebrafish intestine. *Neurogastroenterol Motil* 24:288-299.

Adelstein RS, and Eisenberg E. 1980. Regulation and kinetics of the actin-myosin-ATP interaction. *Annu Rev Biochem* 49:921-956.

Berman HM, Westbrook J, Feng Z, Gilliland G, Bhat TN, Weissig H, Shindyalov IN, and Bourne PE. 2000. The Protein Data Bank. *Nucleic Acids Res* 28:235-242.

Bertini I, Giachetti A, Luchinat C, Parigi G, Petoukhov MV, Pierattelli R, Ravera E, and Svergun DI. 2010. Conformational Space of Flexible Biological Macromolecules from Average Data. *Journal of the American Chemical Society* 132:13553-13558.

Burstein EA, and Emelyanenko VI. 1996. Log-normal description of fluorescence spectra of organic fluorophores. *Photochem Photobiol* 64:316-320.

Campen A, Williams RM, Brown CJ, Meng J, Uversky VN, and Dunker AK. 2008. TOP-IDP-scale: a new amino acid scale measuring propensity for intrinsic disorder. *Protein Pept Lett* 15:956-963.

Cheng Y, Oldfield CJ, Meng J, Romero P, Uversky VN, and Dunker AK. 2007. Mining alpha-helix-forming molecular recognition features with cross species sequence alignments. *Biochemistry* 46:13468-13477.

Czurylo EA, Emelyanenko VI, Permyakov EA, and Dabrowska R. 1991. Spectrofluorimetric studies on C-terminal 34 kDa fragment of caldesmon. *Biophys Chem* 40:181-188.

Czurylo EA, and Kulikova N. 2012. *Anatromy and Physiology of Proteins: Caldesmon*. New York: Nova Science Publishers.

510 Czurylo EA, Zborowski J, and Dabrowska R. 1993. Interaction of Caldesmon with
511 Phospholipids. *Biochemical Journal* 291:403-408.
512 Daughdrill GW, Pielak GJ, Uversky VN, Cortese MS, and Dunker AK. 2005. Natively
513 disordered proteins. In: Buchner J, and Kiefhaber T, eds. *Handbook of Protein Folding*.
514 Weinheim, Germany: Wiley-VCH, Verlag GmbH & Co., 271-353.
515 Di Domenico T, Walsh I, Martin AJ, and Tosatto SC. 2012. MobiDB: a comprehensive database
516 of intrinsic protein disorder annotations. *Bioinformatics* 28:2080-2081.
517 Disfani FM, Hsu WL, Mizianty MJ, Oldfield CJ, Xue B, Dunker AK, Uversky VN, and Kurgan
518 L. 2012. MoRFpred, a computational tool for sequence-based prediction and
519 characterization of short disorder-to-order transitioning binding regions in proteins.
520 *Bioinformatics* 28:i75-83.
521 Dosztanyi Z, Chen J, Dunker AK, Simon I, and Tompa P. 2006. Disorder and sequence repeats
522 in hub proteins and their implications for network evolution. *J Proteome Res* 5:2985-
523 2995.
524 Dosztanyi Z, Csizmok V, Tompa P, and Simon I. 2005a. IUPred: web server for the prediction of
525 intrinsically unstructured regions of proteins based on estimated energy content.
526 *Bioinformatics* 21:3433-3434.
527 Dosztanyi Z, Csizmok V, Tompa P, and Simon I. 2005b. The pairwise energy content estimated
528 from amino acid composition discriminates between folded and intrinsically unstructured
529 proteins. *J Mol Biol* 347:827-839.
530 Dosztanyi Z, Meszaros B, and Simon I. 2009. ANCHOR: web server for predicting protein
531 binding regions in disordered proteins. *Bioinformatics* 25:2745-2746.

532 Dunker AK, Babu M, Barbar E, Blackledge M, Bondos SE, Dosztányi Z, Dyson HJ, Forman-
533 Kay J, Fuxreiter M, Gsponer J, Han K-H, Jones DT, Longhi S, Metallo SJ, Nishikawa K,
534 Nussinov R, Obradovic Z, Pappu R, Rost B, Selenko P, Subramaniam V, Sussman JL,
535 Tompa P, and Uversky VN. 2013. What's in a name? Why these proteins are intrinsically
536 disordered. *Intrinsically Disordered Proteins* 1:e24157.
537 Dunker AK, Brown CJ, Lawson JD, Iakoucheva LM, and Obradovic Z. 2002a. Intrinsic disorder
538 and protein function. *Biochemistry* 41:6573-6582.
539 Dunker AK, Brown CJ, and Obradovic Z. 2002b. Identification and functions of usefully
540 disordered proteins. *Adv Protein Chem* 62:25-49.
541 Dunker AK, Cortese MS, Romero P, Iakoucheva LM, and Uversky VN. 2005. Flexible nets. The
542 roles of intrinsic disorder in protein interaction networks. *Febs J* 272:5129-5148.
543 Dunker AK, Garner E, Guilliot S, Romero P, Albrecht K, Hart J, Obradovic Z, Kissinger C, and
544 Villafranca JE. 1998. Protein disorder and the evolution of molecular recognition: theory,
545 predictions and observations. *Pac Symp Biocomput*:473-484.
546 Dunker AK, Lawson JD, Brown CJ, Williams RM, Romero P, Oh JS, Oldfield CJ, Campen AM,
547 Ratliff CM, Hipps KW, Ausio J, Nissen MS, Reeves R, Kang C, Kissinger CR, Bailey
548 RW, Griswold MD, Chiu W, Garner EC, and Obradovic Z. 2001. Intrinsically disordered
549 protein. *J Mol Graph Model* 19:26-59.
550 Dunker AK, Obradovic Z, Romero P, Garner EC, and Brown CJ. 2000. Intrinsic protein disorder
551 in complete genomes. *Genome Inform Ser Workshop Genome Inform* 11:161-171.
552 Dunker AK, Oldfield CJ, Meng J, Romero P, Yang JY, Chen JW, Vacic V, Obradovic Z, and
553 Uversky VN. 2008a. The unfoldomics decade: an update on intrinsically disordered
554 proteins. *BMC Genomics* 9 Suppl 2:S1.

555 Dunker AK, Silman I, Uversky VN, and Sussman JL. 2008b. Function and structure of
556 inherently disordered proteins. *Curr Opin Struct Biol* 18:756-764.
557 Dunker AK, and Uversky VN. 2008. Signal transduction via unstructured protein conduits. *Nat*
558 *Chem Biol* 4:229-230.
559 Dyson HJ. 2011. Expanding the proteome: disordered and alternatively folded proteins. *Q Rev*
560 *Biophys* 44:467-518.
561 Dyson HJ, and Wright PE. 2002. Coupling of folding and binding for unstructured proteins. *Curr*
562 *Opin Struct Biol* 12:54-60.
563 Dyson HJ, and Wright PE. 2005. Intrinsically unstructured proteins and their functions. *Nat Rev*
564 *Mol Cell Biol* 6:197-208.
565 Ekman D, Light S, Bjorklund AK, and Elofsson A. 2006. What properties characterize the hub
566 proteins of the protein-protein interaction network of Saccharomyces cerevisiae? *Genome*
567 *Biol* 7:R45.
568 Fan X, and Kurgan L. 2014. Accurate prediction of disorder in protein chains with a
569 comprehensive and empirically designed consensus. *J Biomol Struct Dyn* 32:448-464.
570 Fraser IDC, Copeland O, Wu B, and Marston SB. 1997. The inhibitory complex of smooth
571 muscle caldesmon with actin and tropomyosin involves three interacting segments of the
572 C-terminal domain 4. *Biochemistry* 36:5483-5492.
573 Graether SP, Heinonen TY, Raharjo WH, Jin JP, and Mak AS. 1997. Tryptophan residues in
574 caldesmon are major determinants for calmodulin binding. *Biochemistry* 36:364-369.
575 Gusev NB. 2001. Some properties of caldesmon and calponin and the participation of these
576 proteins in regulation of smooth muscle contraction and cytoskeleton formation.
577 *Biochemistry-Moscow* 66:1112-1121.

578 Haynes C, Oldfield CJ, Ji F, Klitgord N, Cusick ME, Radivojac P, Uversky VN, Vidal M, and
579 Iakoucheva LM. 2006. Intrinsic disorder is a common feature of hub proteins from four
580 eukaryotic interactomes. *PLoS Comput Biol* 2:e100.
581 Helfman DM, Levy ET, Berthier C, Shtutman M, Riveline D, Grosheva I, Lachish-Zalait A,
582 Elbaum M, and Bershadsky AD. 1999. Caldesmon inhibits nonmuscle cell contractility
583 and interferes with the formation of focal adhesions. *Mol Biol Cell* 10:3097-3112.
584 Heller WT. 2005. Influence of multiple well defined conformations on small-angle scattering of
585 proteins in solution. *Acta Crystallographica Section D-Biological Crystallography* 61:33-
586 44.
587 Huber PAJ, ElMezgueldi M, Grabarek Z, Slatter DA, Levine BA, and Marston SB. 1996.
588 Multiple-sited interaction of caldesmon with Ca2(+)-calmodulin. *Biochemical Journal*
589 316:413-420.
590 Iakoucheva LM, Radivojac P, Brown CJ, O'Connor TR, Sikes JG, Obradovic Z, and Dunker AK.
591 2004. The importance of intrinsic disorder for protein phosphorylation. *Nucleic Acids Res*
592 32:1037-1049.
593 Ishida T, and Kinoshita K. 2007. PrDOS: prediction of disordered protein regions from amino
594 acid sequence. *Nucleic Acids Res* 35:W460-464.
595 Kordowska J, Huang R, and Wang CL. 2006. Phosphorylation of caldesmon during smooth
596 muscle contraction and cell migration or proliferation. *J Biomed Sci* 13:159-172.
597 Kursula P. 2014. The many structural faces of calmodulin: a multitasking molecular jackknife.
598 *Amino Acids* 46:2295-2304.
599 Kuznicki J, and Filipek A. 1987. Purification and Properties of a Novel Ca2+-Binding Protein
600 (10.5 Kda) from Ehrlich-Ascites-Tumor Cells. *Biochemical Journal* 247:663-667.

601 Li W, Wang W, and Takada S. 2014. Energy landscape views for interplays among folding,
602 binding, and allostery of calmodulin domains. *Proc Natl Acad Sci U S A* 111:10550-
603 10555.
604 Linding R, Jensen LJ, Diella F, Bork P, Gibson TJ, and Russell RB. 2003a. Protein disorder
605 prediction: implications for structural proteomics. *Structure* 11:1453-1459.
606 Linding R, Russell RB, Neduva V, and Gibson TJ. 2003b. GlobPlot: exploring protein sequences
607 for globularity and disorder. *Nucleic Acids Res* 31:3701-3708.
608 Mabuchi K, Li Y, Tao T, and Wang CL. 1996. Immunocytochemical localization of caldesmon
609 and calponin in chicken gizzard smooth muscle. *J Muscle Res Cell Motil* 17:243-260.
610 Makowski P, Makuch R, Sikorski AF, Jezierski A, Pikula S, and Dabrowska R. 1997. Interaction
611 of caldesmon with endoplasmic reticulum membrane: effects on the mobility of
612 phospholipids in the membrane and on the phosphatidylserine base-exchange reaction.
613 *Biochemical Journal* 328:505-509.
614 Mani RS, and Kay CM. 1996. Calcium binding proteins. In: Barany M, ed. *Biochemistry of*
615 *Smooth Muscle Contraction*. New York: Academic Press, 105-116.
616 Marquardt DW. 1963. An algorithm for least-squares estimation of nonlinear parameters. *J Soc*
617 *Indust Appl Math* 11:431-441.
618 Marston SB, Fraser ID, Huber PA, Pritchard K, Gusev NB, and Torok K. 1994. Location of two
619 contact sites between human smooth muscle caldesmon and Ca(2+)-calmodulin. *J Biol*
620 *Chem* 269:8134-8139.
621 Marston SB, and Redwood CS. 1991. The molecular anatomy of caldesmon. *Biochem J* 279 (Pt
622 1):1-16.

623 Martson SB, and Huber PAJ. 1996. Caldesmon. In: Barany M, ed. *Biochemistry of Smooth*
624 *Muscle Contraction*. New York: Academic Press, 70-90.
625 Matsumura F, and Yamashiro S. 1993. Caldesmon. *Curr Opin Cell Biol* 5:70-76.
626 Medvedeva MV, Kolobova EA, Huber PAJ, Fraser IDC, Marston SB, and Gusev NB. 1997.
627 Mapping of contact sites in the caldesmon-calmodulin complex. *Biochemical Journal*
628 324:255-262.
629 Meszaros B, Simon I, and Dosztanyi Z. 2009. Prediction of protein binding regions in disordered
630 proteins. *PLoS Comput Biol* 5:e1000376.
631 Mezgueldi M, Derancourt J, Calas B, Kassab R, and Fattoum A. 1994. Precise identification of
632 the regulatory F-actin- and calmodulin-binding sequences in the 10-kDa carboxyl-
633 terminal domain of caldesmon. *J Biol Chem* 269:12824-12832.
634 Mohan A, Oldfield CJ, Radivojac P, Vacic V, Cortese MS, Dunker AK, and Uversky VN. 2006.
635 Analysis of molecular recognition features (MoRFs). *J Mol Biol* 362:1043-1059.
636 Moroz OV, Moroz YS, Wu Y, Olsen AB, Cheng H, Mack KL, McLaughlin JM, Raymond EA,
637 Zhezherya K, Roder H, and Korendovych IV. 2013. A single mutation in a regulatory
638 protein produces evolvable allosterically regulated catalyst of nonnatural reaction. *Angew*
639 *Chem Int Ed Engl* 52:6246-6249.
640 Oates ME, Romero P, Ishida T, Ghalwash M, Mizianty MJ, Xue B, Dosztanyi Z, Uversky VN,
641 Obradovic Z, Kurgan L, Dunker AK, and Gough J. 2013. D(2)P(2): database of
642 disordered protein predictions. *Nucleic Acids Res* 41:D508-516.
643 Obradovic Z, Peng K, Vucetic S, Radivojac P, and Dunker AK. 2005. Exploiting heterogeneous
644 sequence properties improves prediction of protein disorder. *Proteins* 61 Suppl 7:176-
645 182.

646 Oldfield CJ, Cheng Y, Cortese MS, Brown CJ, Uversky VN, and Dunker AK. 2005a. Comparing
647 and combining predictors of mostly disordered proteins. *Biochemistry* 44:1989-2000.
648 Oldfield CJ, Cheng Y, Cortese MS, Romero P, Uversky VN, and Dunker AK. 2005b. Coupled
649 folding and binding with alpha-helix-forming molecular recognition elements.
650 *Biochemistry* 44:12454-12470.
651 Pace CN, Vajdos F, Fee L, Grimsley G, and Gray T. 1995. How to Measure and Predict the
652 Molar Absorption-Coefficient of a Protein. *Protein Science* 4:2411-2423.
653 Patil A, and Nakamura H. 2006. Disordered domains and high surface charge confer hubs with
654 the ability to interact with multiple proteins in interaction networks. *FEBS Lett* 580:2041-
655 2045.
656 Pejaver V, Hsu WL, Xin F, Dunker AK, Uversky VN, and Radivojac P. 2014. The structural and
657 functional signatures of proteins that undergo multiple events of post-translational
658 modification. *Protein Sci* 23:1077-1093.
659 Peng K, Radivojac P, Vucetic S, Dunker AK, and Obradovic Z. 2006a. Length-dependent
660 prediction of protein intrinsic disorder. *Bmc Bioinformatics* 7.
661 Peng K, Radivojac P, Vucetic S, Dunker AK, and Obradovic Z. 2006b. Length-dependent
662 prediction of protein intrinsic disorder. *BMC Bioinformatics* 7:208.
663 Peng K, Vucetic S, Radivojac P, Brown CJ, Dunker AK, and Obradovic Z. 2005. Optimizing
664 long intrinsic disorder predictors with protein evolutionary information. *J Bioinform*
665 *Comput Biol* 3:35-60.
666 Peng ZL, and Kurgan L. 2012. Comprehensive comparative assessment of in-silico predictors of
667 disordered regions. *Curr Protein Pept Sci* 13:6-18.

668 Permyakov EA, and Burstein EA. 1984. Some aspects of studies of thermal transitions in
669 proteins by means of their intrinsic fluorescence. *Biophys Chem* 19:265-271.
670 Permyakov EA, Burstein EA, Sawada Y, and Yamazaki I. 1977. Luminescence of
671 phenylalamine residues in superoxide dismutase from green pea. *Biochim Biophys Acta*
672 491:149-154.
673 Permyakov SE, Millett IS, Doniach S, Permyakov EA, and Uversky VN. 2003. Natively
674 unfolded C-terminal domain of caldesmon remains substantially unstructured after the
675 effective binding to calmodulin. *Proteins* 53:855-862.
676 Polyakov AA, Huber PAJ, Marston SB, and Gusev NB. 1998. Interaction of isoforms of S100
677 protein with smooth muscle caldesmon. *Febs Letters* 422:235-239.
678 Potenza E, Domenico TD, Walsh I, and Tosatto SC. 2015. MobiDB 2.0: an improved database of
679 intrinsically disordered and mobile proteins. *Nucleic Acids Res*.
680 Prilusky J, Felder CE, Zeev-Ben-Mordehai T, Rydberg EH, Man O, Beckmann JS, Silman I, and
681 Sussman JL. 2005. FoldIndex: a simple tool to predict whether a given protein sequence
682 is intrinsically unfolded. *Bioinformatics* 21:3435-3438.
683 Privalov PL. 1979. Stability of proteins: small globular proteins. *Adv Protein Chem* 33:167-241.
684 Privalov PL, and Potekhin SA. 1986. Scanning microcalorimetry in studying temperature-
685 induced changes in proteins. *Methods Enzymol* 131:4-51.
686 Radivojac P, Iakoucheva LM, Oldfield CJ, Obradovic Z, Uversky VN, and Dunker AK. 2007.
687 Intrinsic disorder and functional proteomics. *Biophys J* 92:1439-1456.
688 Romero P, Obradovic Z, Li X, Garner EC, Brown CJ, and Dunker AK. 2001. Sequence
689 complexity of disordered protein. *Proteins* 42:38-48.

690 Shirinsky VP, Bushueva TL, and Frolova SI. 1988. Caldesmon-calmodulin interaction. Study by
691 the method of protein intrinsic tryptophan fluorescence. *Biochem J* 255:203-208.
692 Shirinsky VP, Vorotnikov AV, and Gusev NB. 1999. Caldesmon phosphorylation and smooth
693 muscle contraction. In: Kohama K, and Sasaki Y, eds. *Molecular Biology of Smooth*
694 *Muscle Contraction*. Austin, TX, USA: R.G. Landes Company, 59-79.
695 Singh GP, Ganapathi M, Sandhu KS, and Dash D. 2006. Intrinsic unstructuredness and
696 abundance of PEST motifs in eukaryotic proteomes. *Proteins* 62:309-315.
697 Sobue K, and Sellers JR. 1991. Caldesmon, a novel regulatory protein in smooth muscle and
698 nonmuscle actomyosin systems. *J Biol Chem* 266:12115-12118.
699 Sulmann S, Dell'Orco D, Marino V, Behnen P, and Koch KW. 2014. Conformational changes in
700 calcium-sensor proteins under molecular crowding conditions. *Chemistry* 20:6756-6762.
701 Szklarczyk D, Franceschini A, Kuhn M, Simonovic M, Roth A, Minguez P, Doerks T, Stark M,
702 Muller J, Bork P, Jensen LJ, and von Mering C. 2011. The STRING database in 2011:
703 functional interaction networks of proteins, globally integrated and scored. *Nucleic Acids*
704 *Res* 39:D561-568.
705 Tokuriki N, Oldfield CJ, Uversky VN, Berezovsky IN, and Tawfik DS. 2009. Do viral proteins
706 possess unique biophysical features? *Trends Biochem Sci* 34:53-59.
707 Tompa P. 2002. Intrinsically unstructured proteins. *Trends Biochem Sci* 27:527-533.
708 Tompa P. 2005. The interplay between structure and function in intrinsically unstructured
709 proteins. *FEBS Lett* 579:3346-3354.
710 Tompa P. 2012. Intrinsically disordered proteins: a 10-year recap. *Trends Biochem Sci* 37:509-
711 516.

712 Tompa P, and Csermely P. 2004. The role of structural disorder in the function of RNA and
713 protein chaperones. *FASEB J* 18:1169-1175.
714 Tompa P, Szasz C, and Buday L. 2005. Structural disorder throws new light on moonlighting.
715 *Trends Biochem Sci* 30:484-489.
716 Turoverov KK, Kuznetsova IM, and Uversky VN. 2010. The protein kingdom extended: ordered
717 and intrinsically disordered proteins, their folding, supramolecular complex formation,
718 and aggregation. *Prog Biophys Mol Biol* 102:73-84.
719 Uversky VN. 2002a. Natively unfolded proteins: a point where biology waits for physics.
720 *Protein Sci* 11:739-756.
721 Uversky VN. 2002b. What does it mean to be natively unfolded? *Eur J Biochem* 269:2-12.
722 Uversky VN. 2003. Protein folding revisited. A polypeptide chain at the folding-misfolding-
723 nonfolding cross-roads: which way to go? *Cell Mol Life Sci* 60:1852-1871.
724 Uversky VN. 2010. The mysterious unfoldome: structureless, underappreciated, yet vital part of
725 any given proteome. *J Biomed Biotechnol* 2010:568068.
726 Uversky VN. 2011a. Intrinsically disordered proteins from A to Z. *Int J Biochem Cell Biol*
727 43:1090-1103.
728 Uversky VN. 2011b. Multitude of binding modes attainable by intrinsically disordered proteins:
729 a portrait gallery of disorder-based complexes. *Chem Soc Rev* 40:1623-1634.
730 Uversky VN. 2012. Disordered competitive recruiter: fast and foldable. *J Mol Biol* 418:267-268.
731 Uversky VN. 2013a. A decade and a half of protein intrinsic disorder: Biology still waits for
732 physics. *Protein Sci* 22:693-724.
733 Uversky VN. 2013b. Intrinsic Disorder-based Protein Interactions and their Modulators. *Curr*
734 *Pharm Des* 19:4191-4213.

735 Uversky VN. 2013c. Unusual biophysics of intrinsically disordered proteins. *Biochim Biophys*
736 *Acta* 1834:932-951.
737 Uversky VN, Dave V, Iakoucheva LM, Malaney P, Metallo SJ, Pathak RR, and Joerger AC.
738 2014. Pathological unfoldomics of uncontrolled chaos: intrinsically disordered proteins
739 and human diseases. *Chem Rev* 114:6844-6879.
740 Uversky VN, and Dunker AK. 2010. Understanding protein non-folding. *Biochim Biophys Acta*
741 1804:1231-1264.
742 Uversky VN, Gillespie JR, and Fink AL. 2000. Why are "natively unfolded" proteins
743 unstructured under physiologic conditions? *Proteins* 41:415-427.
744 Uversky VN, Oldfield CJ, and Dunker AK. 2005. Showing your ID: intrinsic disorder as an ID
745 for recognition, regulation and cell signaling. *J Mol Recognit* 18:343-384.
746 Uversky VN, Oldfield CJ, and Dunker AK. 2008. Intrinsically disordered proteins in human
747 diseases: introducing the D2 concept. *Annu Rev Biophys* 37:215-246.
748 Vacic V, Oldfield CJ, Mohan A, Radivojac P, Cortese MS, Uversky VN, and Dunker AK.
749 2007a. Characterization of molecular recognition features, MoRFs, and their binding
750 partners. *J Proteome Res* 6:2351-2366.
751 Vacic V, Uversky VN, Dunker AK, and Lonardi S. 2007b. Composition Profiler: a tool for
752 discovery and visualization of amino acid composition differences. *BMC Bioinformatics*
753 8:211.
754 Vorotnikov AV, Bogatcheva NV, and Gusev NB. 1992. Caldesmon Phospholipid Interaction -
755 Effect of Protein-Kinase-C Phosphorylation and Sequence Similarity with Other
756 Phospholipid-Binding Proteins. *Biochemical Journal* 284:911-916.

757 Vorotnikov AV, and Gusev NB. 1990. Interaction of Smooth-Muscle Caldesmon with
758 Phospholipids. *FEBS Letters* 277:134-136.
759 Vucetic S, Xie H, Iakoucheva LM, Oldfield CJ, Dunker AK, Obradovic Z, and Uversky VN.
760 2007. Functional anthology of intrinsic disorder. 2. Cellular components, domains,
761 technical terms, developmental processes, and coding sequence diversities correlated
762 with long disordered regions. *J Proteome Res* 6:1899-1916.
763 Walsh I, Martin AJ, Di Domenico T, and Tosatto SC. 2012. ESpritz: accurate and fast prediction
764 of protein disorder. *Bioinformatics* 28:503-509.
765 Wang CL, Chalovich JM, Graceffa P, Lu RC, Mabuchi K, and Stafford WF. 1991. A long helix
766 from the central region of smooth muscle caldesmon. *J Biol Chem* 266:13958-13963.
767 Wang EZ, Zhuang SB, Kordowska J, Grabarek Z, and Wang CLA. 1997. Calmodulin binds to
768 caldesmon in an antiparallel manner. *Biochemistry* 36:15026-15034.
769 Ward JJ, Sodhi JS, McGuffin LJ, Buxton BF, and Jones DT. 2004. Prediction and functional
770 analysis of native disorder in proteins from the three kingdoms of life. *J Mol Biol*
771 337:635-645.
772 Wright PE, and Dyson HJ. 1999. Intrinsically unstructured proteins: re-assessing the protein
773 structure-function paradigm. *J Mol Biol* 293:321-331.
774 Xie H, Vucetic S, Iakoucheva LM, Oldfield CJ, Dunker AK, Obradovic Z, and Uversky VN.
775 2007a. Functional anthology of intrinsic disorder. 3. Ligands, post-translational
776 modifications, and diseases associated with intrinsically disordered proteins. *J Proteome*
777 *Res* 6:1917-1932.

778 Xie H, Vucetic S, Iakoucheva LM, Oldfield CJ, Dunker AK, Uversky VN, and Obradovic Z.
779 2007b. Functional anthology of intrinsic disorder. 1. Biological processes and functions
780 of proteins with long disordered regions. *J Proteome Res* 6:1882-1898.
781 Xue B, Dunbrack RL, Williams RW, Dunker AK, and Uversky VN. 2010a. PONDR-FIT: a
782 meta-predictor of intrinsically disordered amino acids. *Biochim Biophys Acta* 1804:996-
783 1010.
784 Xue B, Dunker AK, and Uversky VN. 2012a. Orderly order in protein intrinsic disorder
785 distribution: disorder in 3500 proteomes from viruses and the three domains of life. *J*
786 *Biomol Struct Dyn* 30:137-149.
787 Xue B, Dunker AK, and Uversky VN. 2012b. Orderly order in protein intrinsic disorder
788 distribution: Disorder in thirty five hundred proteomes from viruses and the three
789 domains of life. *Journal of Biomolecular Structure and Dynamics*:In press.
790 Xue B, Williams RW, Oldfield CJ, Dunker AK, and Uversky VN. 2010b. Archaic chaos:
791 intrinsically disordered proteins in Archaea. *BMC Syst Biol* 4 Suppl 1:S1.
792 Yamada Y, Matsuo T, Iwamoto H, and Yagi N. 2012. A Compact Intermediate State of
793 Calmodulin in the Process of Target Binding. *Biochemistry* 51:3963-3970.
794 Yang ZR, Thomson R, McNeil P, and Esnouf RM. 2005. RONN: the bio-basis function neural
795 network technique applied to the detection of natively disordered regions in proteins.
796 *Bioinformatics* 21:3369-3376.
797 Zhan QQ, Wong SS, and Wang CL. 1991. A calmodulin-binding peptide of caldesmon. *J Biol*
798 *Chem* 266:21810-21814.
799
800

Table 1(on next page)

Equilibrium association constants (K_{CaM}) for complexes between CaM and wild type CaD_{136} and its mutants and their relative fluorescence quantum yields in free and CaM-bound states.

Table 1. Equilibrium association constants (K_{CaM}) for complexes between CaM and wild type CaD_{136} and its mutants and their relative fluorescence quantum yields in the free and CaM-bound states.

Table 1. Equilibrium association constants (K_{CaM}) for complexes between CaM and wild type CaD_{136} and its mutants and their relative fluorescence quantum yields in the free and CaM-bound states.

Protein	K_{CaM}	Q/Q_{trp} (in solution)	Q/Q_{trp} (in complex with calmodulin)
WT	$(6.5\pm1.6)\times10^5$	1.25	2.40
W674A	$(2.2\pm0.6)\times10^5$	1.25	2.72
W707A	$(3.0\pm0.8)\times10^5$	1.50	2.55
W737A	$(1.8\pm0.5)\times10^6$	1.49	2.95
Double mutant	$(4.4\pm1.1)\times10^4$	1.19	2.64

1

Evaluating the intrinsic disorder propensities of chicken CaD (A), CaD_{136} (B), and chicken CaM (C) by the family of PONDR predictors.

Figure 1. Evaluating the intrinsic disorder propensities of chicken CaD (**A**), CaD_{136} (**B**), and chicken CaM (**C**) by the family of PONDR predictors. A disorder threshold is indicated as a thin line (at score = 0.5) in all plots to show a boundary between disorder (>0.5) and order (<0.5). Plot **D** represents the amino acid sequences of CaD_{136} and CaM, for which the positively and negatively charged residues are highlighted. The positions of tryptophan residues within the CaD_{136} sequence are also indicated. mp&#65533;rS&#65533;f&#65533;&#65533;

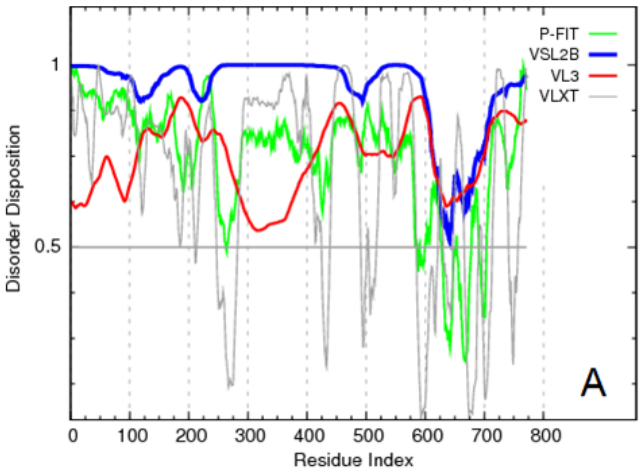

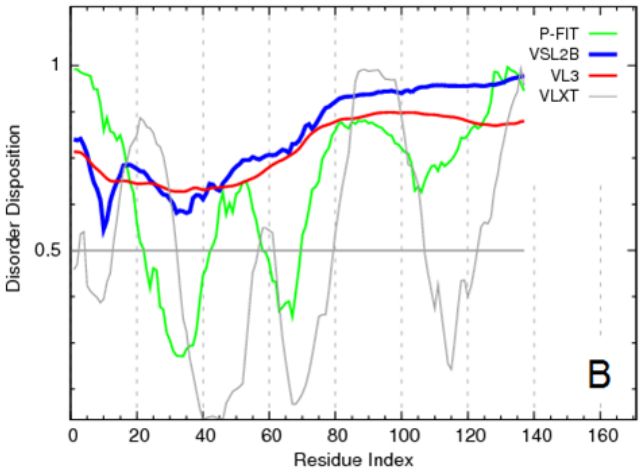

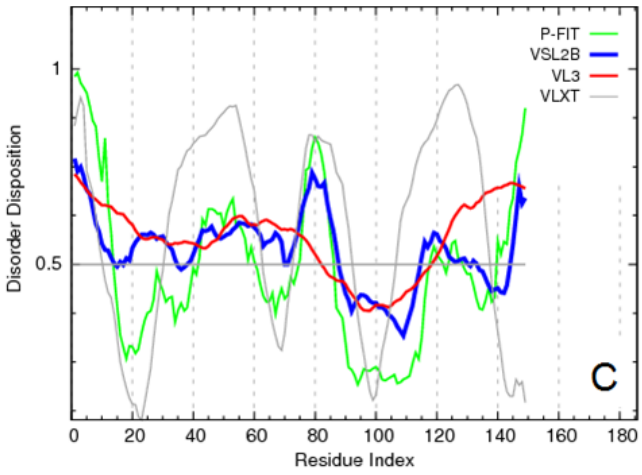

>sp|P12957|CALD1_CHICK Caldesmon OS=Gallus gallus GN=CALD1 PE=1 SV=2 635-771 fragment

SRLEQYTSAVVGNKAAKPAKPAASDLPVPAEGVRNIKSMMEKGNVFSSPG
GTGTPNKETAGLKVGVSSRINEMLTKTPEGNKSPAPKPSDLRPGDVSGKR
NLMEKQSVEKPAASSSKVTATGKKSETNGLRQFEKEP

>sp|P62149|CALM_CHICK Calmodulin OS=Gallus gallus GN=CALM PE=1 SV=2

MADQLTEEQIAEFKEAFSLFDKDGDGTITTKELGTVMRSLGQNPTEAELQ
DMINEVDADGNGTIDFPEFLTMMARKMKDTDSEEEIREAFRVFDKDGNGY
ISAAELRHVMTNLGEKLTDEEVDEMIREADIDGDGQVNYEEFVQMMTAK

D

2

Evaluation of the functional intrinsic disorder propensity of the human CaD (UniProt ID: Q05682) by the D^2P^2 platform.

Figure 2. Evaluation of the functional intrinsic disorder propensity of the human CaD (UniProt ID: Q05682) by the D^2P^2 platform (http://d2p2.pro/) (Oates et al. 2013) . In this plot, top nine colored bars represent location of disordered regions predicted by different computational tools (Espritz-D, Espritz-N, Espritz-X, IUPred-L, IUPred-S, PV2, PrDOS, PONDR® VSL2b, and PONDR® VLXT, see keys for the corresponding color codes). Dark red bar shows the location of the functional domain found by the Pfam platform, which is a database ofprotein familiesthat includes their annotations andmultiple sequence alignmentsgenerated usinghidden Markov models (Bateman et al. 2004; Finn et al. 2006; Finn et al. 2008) . Green-and-white bar in the middle of the plot shows the predicted disorder agreement between these nine predictors, with green parts corresponding to disordered regions by consensus. Red, yellow and purple circles at the bottom of the plot show the locations of phosphorylation, acetylation and ubiquitination sites, respectively. **B**. Analysis of the interactivity of the chicken gizzard CaD (UniProt ID: P12957) by STRING (Szklarczyk et al. 2011) . STRING produces the network of predicted associations for a particular group of proteins. The network nodes are proteins, whereas the edges represent the predicted or known functional associations. An edge may be drawn with up to 7 differently colored lines that represent the existence of the seven types of evidence used in predicting the associations. A red line indicates the presence of fusion evidence; a green line - neighborhood evidence; a blue line – co-occurrence evidence; a purple line - experimental evidence; a yellow line – text mining evidence; a light blue line - database evidence; a black line – co-expression evidence (Szklarczyk et al. 2011) .

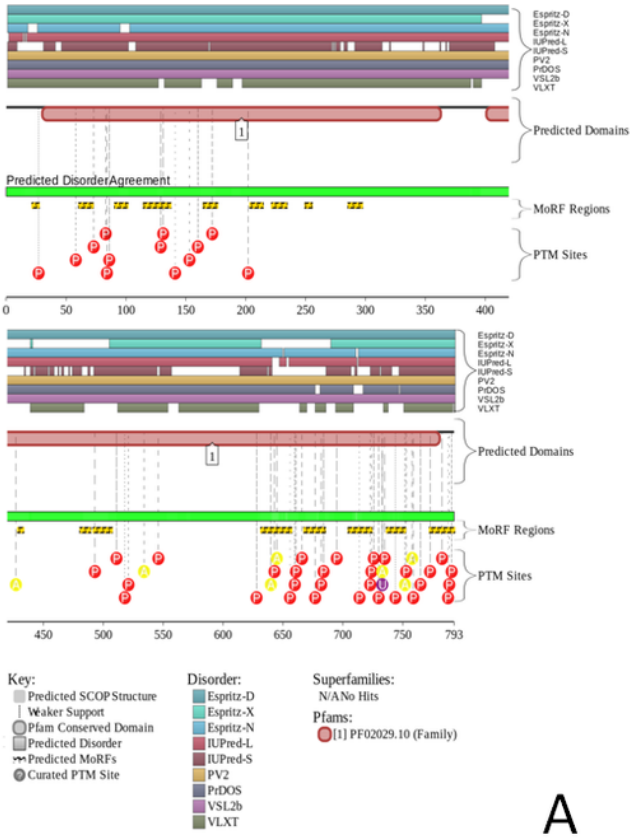
Espritz-D
Espritz-X
Espritz-N
IUPred-L
IUPred-S
PV2
PrDOS
VSL2b
VLXT
Predicted Domains
Predicted DisorderAgreement
MoRF Regions
PTM Sites
0
50
100
150
200
250
300
350
400
450
500
550
600
650
700
750
793
Key:
Predicted SCOP Structure
Weaker Support
Pfam Conserved Domain
Predicted Disorder
Predicted MoRFs
Curated PTM Site
Disorder:
Espritz-D
Espritz-X
Espritz-N
IUPred-L
IUPred-S
PV2
PrDOS
VSL2b
VLXT
Superfamilies:
N/ANo Hits
Pfams:
[1] PF02029.10 (Family)

A

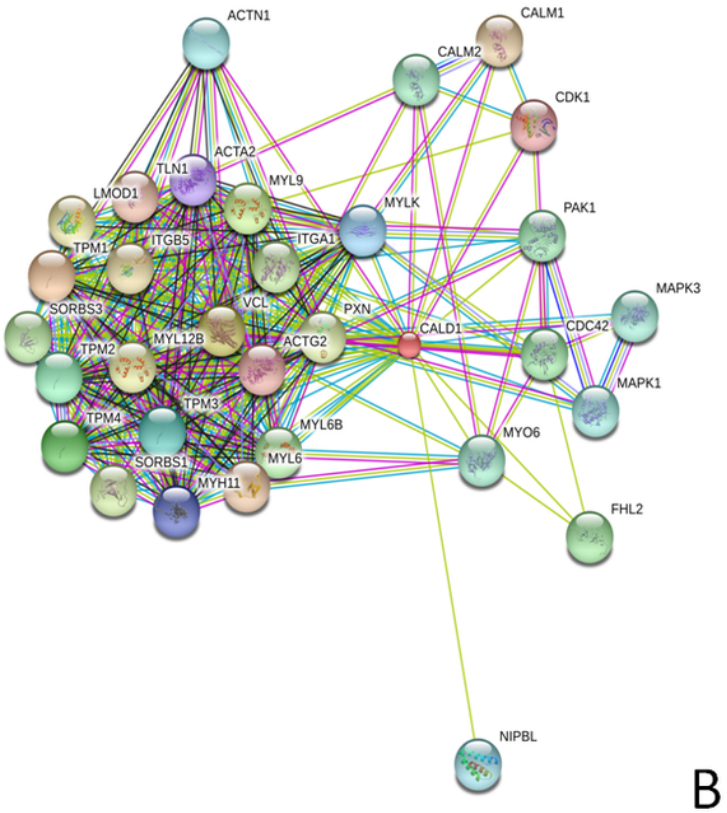
ACTN1
CALM1
CALM2
CDK1
ACTA2
TLN1
MYL9
LMOD1
MYLK
PAK1
TPM1
ITGB5
ITGA1
MAPK3
SORBS3
VCL
PXN
CALD1
CDC42
MYL12B
ACTG2
TPM2
MAPK1
TPM3
TPM4
MYL6B
MYO6
SORBS1
MYL6
MYH11
FHL2
NIPBL

B

3

Evaluation of the functional intrinsic disorder propensity of human CaM (UniProt ID: P62158) by D^2P^2 database.

Figure 3. Evaluation of the functional intrinsic disorder propensity of human CaM (UniProt ID: P62158) by D^2P^2 database (http://d2p2.pro/) (Oates et al. 2013) . In this plot, top dark blue bar with green stripes shows the localization of disordered region annotated in the IDEAL database (Fukuchi et al. 2012) for this protein. Next nine colored bars represent location of disordered regions predicted by different disorder predictors (Espritz-D, Espritz-N, Espritz-X, IUPred-L, IUPred-S, PV2, PrDOS, PONDR® VSL2b, and PONDR® VLXT, see keys for the corresponding color codes). Dark red bar shows the location of the functional domain found by the Pfam platform, which is a database ofprotein familiesthat includes their annotations andmultiple sequence alignmentsgenerated usinghidden Markov models. (Bateman et al. 2004; Finn et al. 2006; Finn et al. 2008) Blue-and-white bar in the middle of the plot shows the predicted disorder agreement between these nine predictors, with green parts corresponding to disordered regions by consensus. Red, yellow, purple and blue circles at the bottom of the plot show the location of phosphorylation, acetylation, ubiquitination, and methylation sites, respectively. **B**. Analysis of the interactivity of the chicken CaM (UniProt ID: P62149) by STRING (Szklarczyk et al. 2011) .

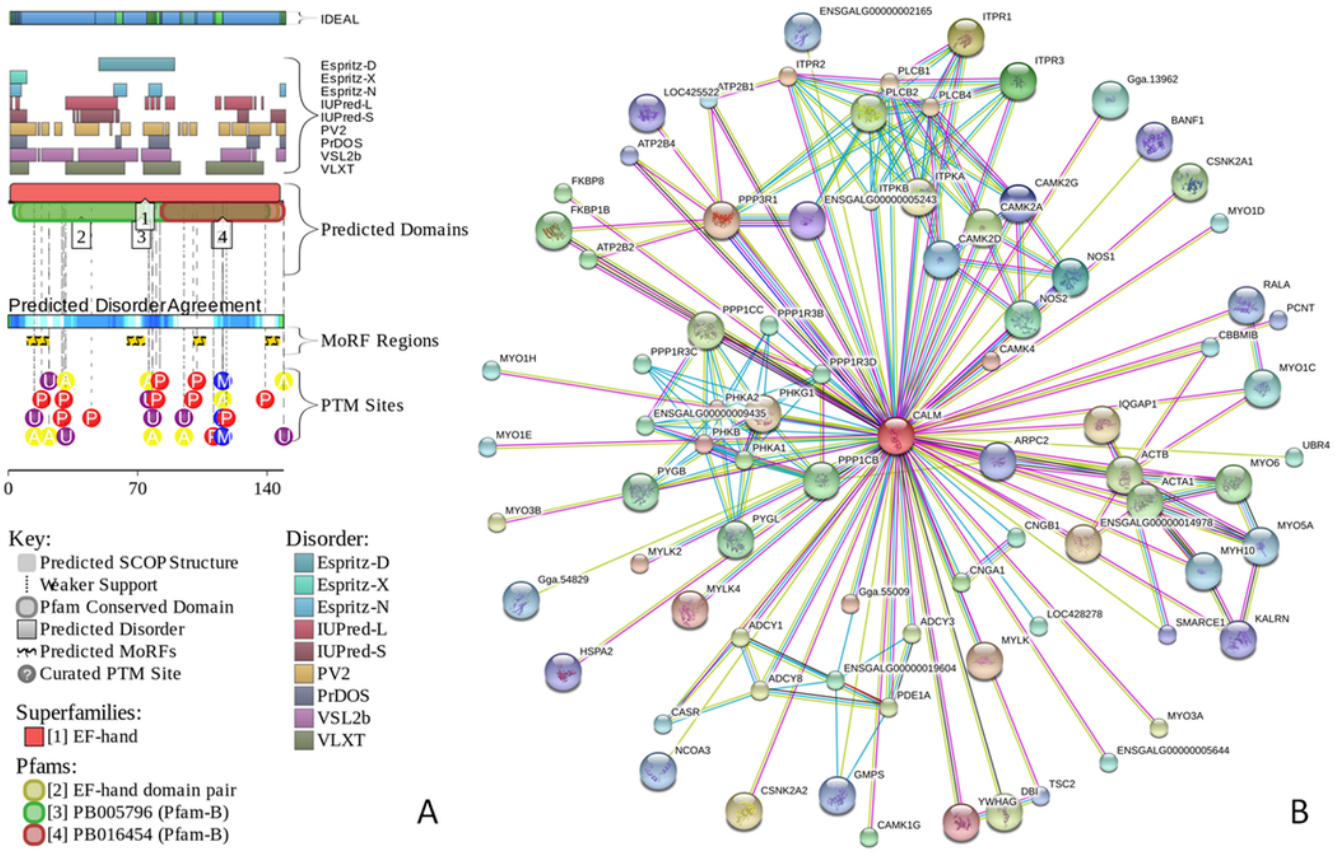
IDEAL
Espritz-D
Espritz-X
Espritz-N
IUPred-L
IUPred-S
PV2
PrDOS
VSL2b
VLXT
Predicted Domains
Predicted Disorder Agreement
MoRF Regions
PTM Sites
0
70
140
Key:
Predicted SCOP Structure
Weaker Support
Pfam Conserved Domain
Predicted Disorder
Predicted MoRFs
Curated PTM Site
Superfamilies:
[1] EF-hand
Pfams:
[2] EF-hand domain pair
[3] PB005796 (Pfam-B)
[4] PB016454 (Pfam-B)
Disorder:
Espritz-D
Espritz-X
Espritz-N
IUPred-L
IUPred-S
PV2
PrDOS
VSL2b
VLXT
A
ENSGALG00000002165
ITPR1
ITPR2
ITPR3
PLCB1
PLCB2
PLCB4
LOC425522
ATP2B1
Gga.13962
BANF1
ATP2B4
CSNK2A1
FKBP8
ITPKB
ITPKA
CAMK2G
FKBP1B
PPP3R1
ENSGALG00000005243
CAMK2A
MYO1D
ATP2B2
CAMK2D
NOS1
NOS2
RALA
PCNT
PPP1CC
PPP1R3B
CBBMIB
MYO1H
PPP1R3C
PPP1R3D
CAMK4
MYO1C
PHKA2
PHKG1
IQGAP1
ENSGALG00000009435
CALM
MYO1E
PHKB
PHKA1
ARPC2
UBR4
ACTB
PYGB
PPP1CB
MYO6
ACTA1
MYO3B
PYGL
CNGB1
ENSGALG00000014978
MYO5A
MYLK2
MYH10
Gga.54829
CNGA1
MYLK4
Gga.55009
LOC428278
ADCY1
ADCY3
SMARCE1
KALRN
HSPA2
MYLK
ENSGALG00000019604
ADCY8
PDE1A
CASR
MYO3A
NCOA3
ENSGALG00000005644
GMPS
TSC2
CSNK2A2
DBI
YWHAG
CAMK1G
B

4

Analysis of the charge distribution on the surface of CaM molecule.

Figure 4. Analysis of the charge distribution on the surface of CaM molecule. PDB file: 1CLM. Analyzed protein: calmodulin, Ca^{2+}-form (1 chain, 4 Ca ions), without first 3 residues Ala, Gln, and Glu and without a last residue Lys. Ca^{2+} ions and water molecules were removed, absent hydrogen atoms were added. Calculations were done using the Swiss-PdbViewer v3.7b2 program. Method of calculation: Poisson-Boltzmann, using partial atom charges, ionic strength 0M or 0.05M, dielectric constant of solvent 80, for protein - 4. Colors: Red - potential value is NEGATIVE, -1.8 kT/e; White - potential value is ZERO; Blue - potential value is POSITIVE, 1.8 kT/e.

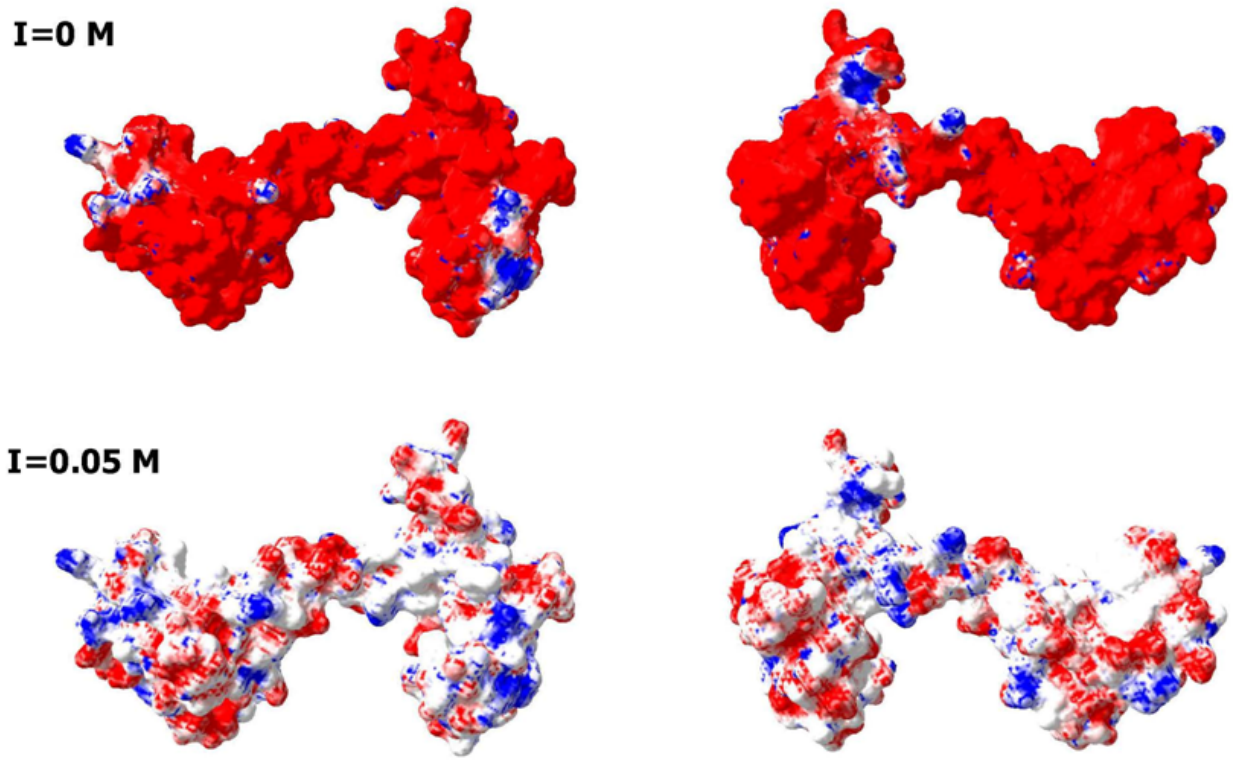
I=0 M
I=0.05 M

5

Computational analysis of the effect of tryptophan mutations on the disorder propensity of CaD_{136}.

Figure 5. Computational analysis of the effect of tryptophan mutations on the disorder propensity of CaD_{136} evaluated by PONDR® VLXT (**A**) and PONDR-FIT (**B**). Locations of the predicted disorder-based binding sites are shown at the bottom of plots as pink (AIBSs), dark green (MoRFpreds), and dark blue (α-MoRFs) bars, respectively.

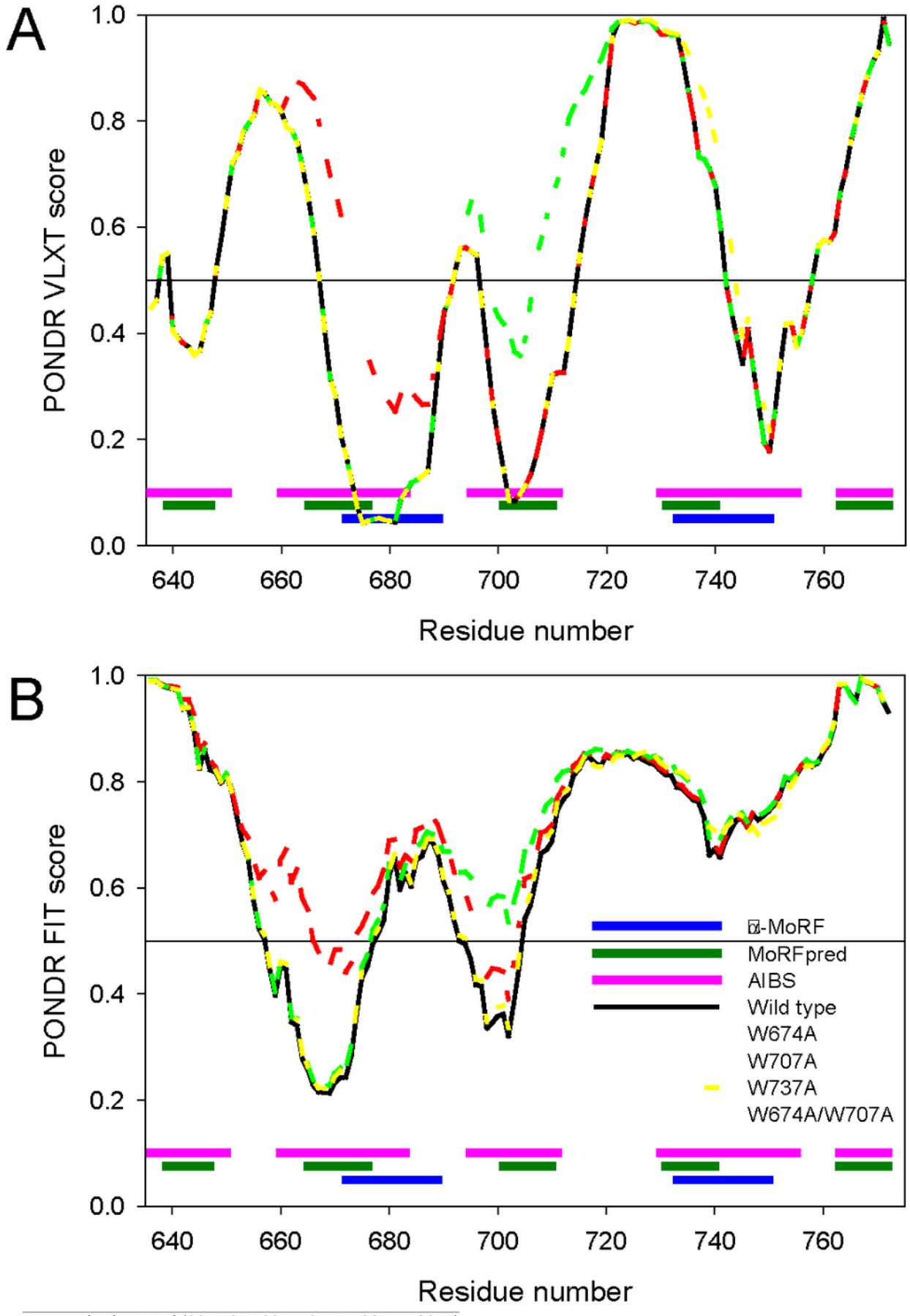
A
PONDR VLXT score
1.0
0.8
0.6
0.4
0.2
0.0
640
660
680
700
720
740
760
Residue number
B
PONDR FIT score
1.0
0.8
0.6
0.4
0.2
0.0
640
660
680
700
720
740
760
Residue number
α-MoRF
MoRFpred
AIBS
Wild type
W674A
W707A
W737A
W674A/W707A

6

Far-UV CD spectra of wild type (1), W674A (2), W707A (3), W737A (4) and W674A/W707A (5) CaD_{136}.

Figure 6. Far-UV CD spectra of wild type (**1**), W674A (**2**), W707A (**3**), W737A (**4**) and W674A/W707A (**5**) CaD_{136}. All measurements were carried out at a protein concentration of 0.6-0.8 mg/ml, cell pathlength 0.1 mm, 15°C.

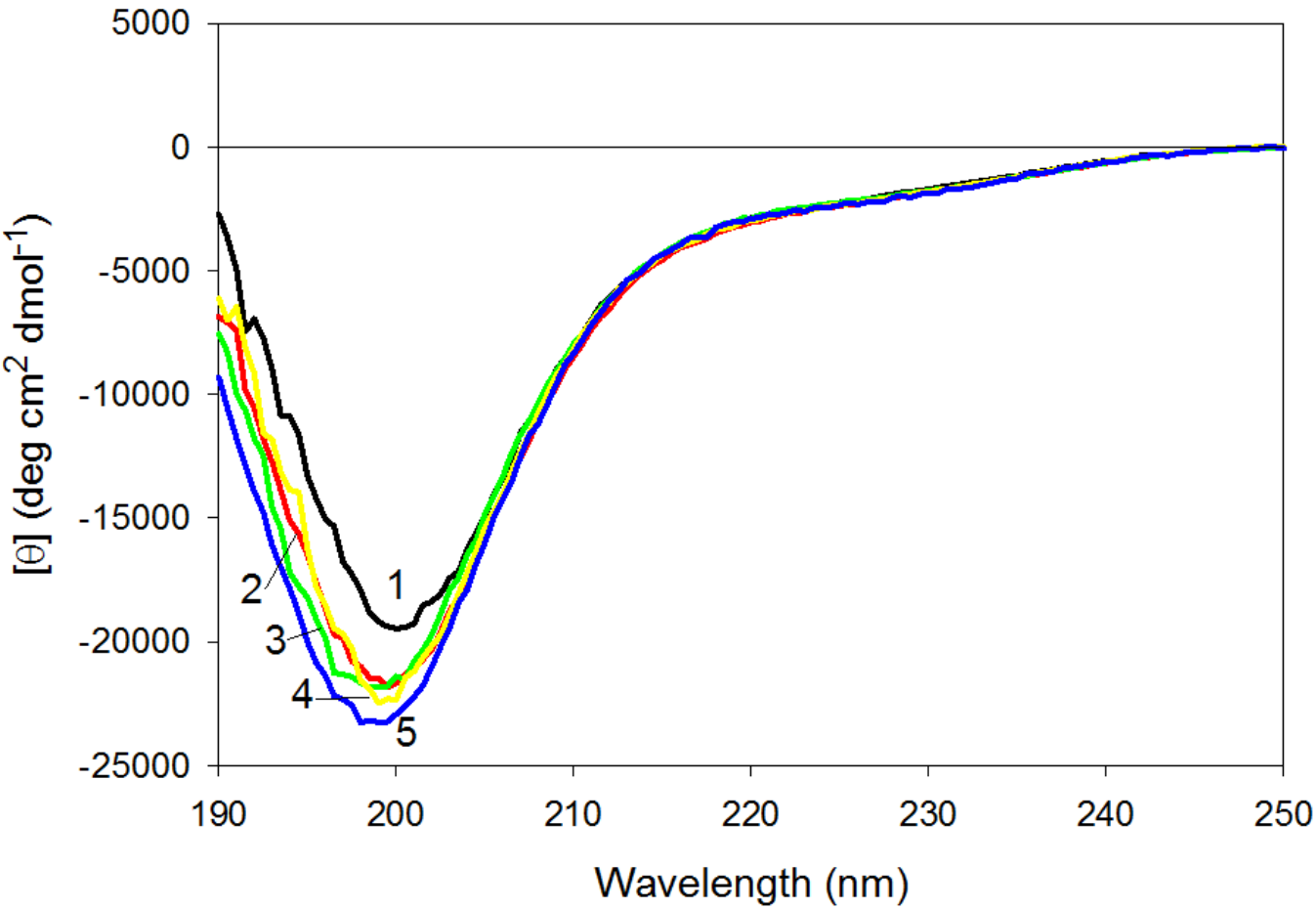

7

Near-UV CD spectra of wild type (1), W674A (2), W707A (3), W737A (4), and W674A/W707A (5) CaD_{136}.

Figure 7. Near-UV CD spectra of wild type (**1**), W674A (**2**), W707A (**3**), W737A (**4**), and W674A/W707A (**5**) CaD_{136}. All measurements were carried out at a protein concentration of 0.6-0.8 mg/ml, cell pathlength 10 mm, 15°C.

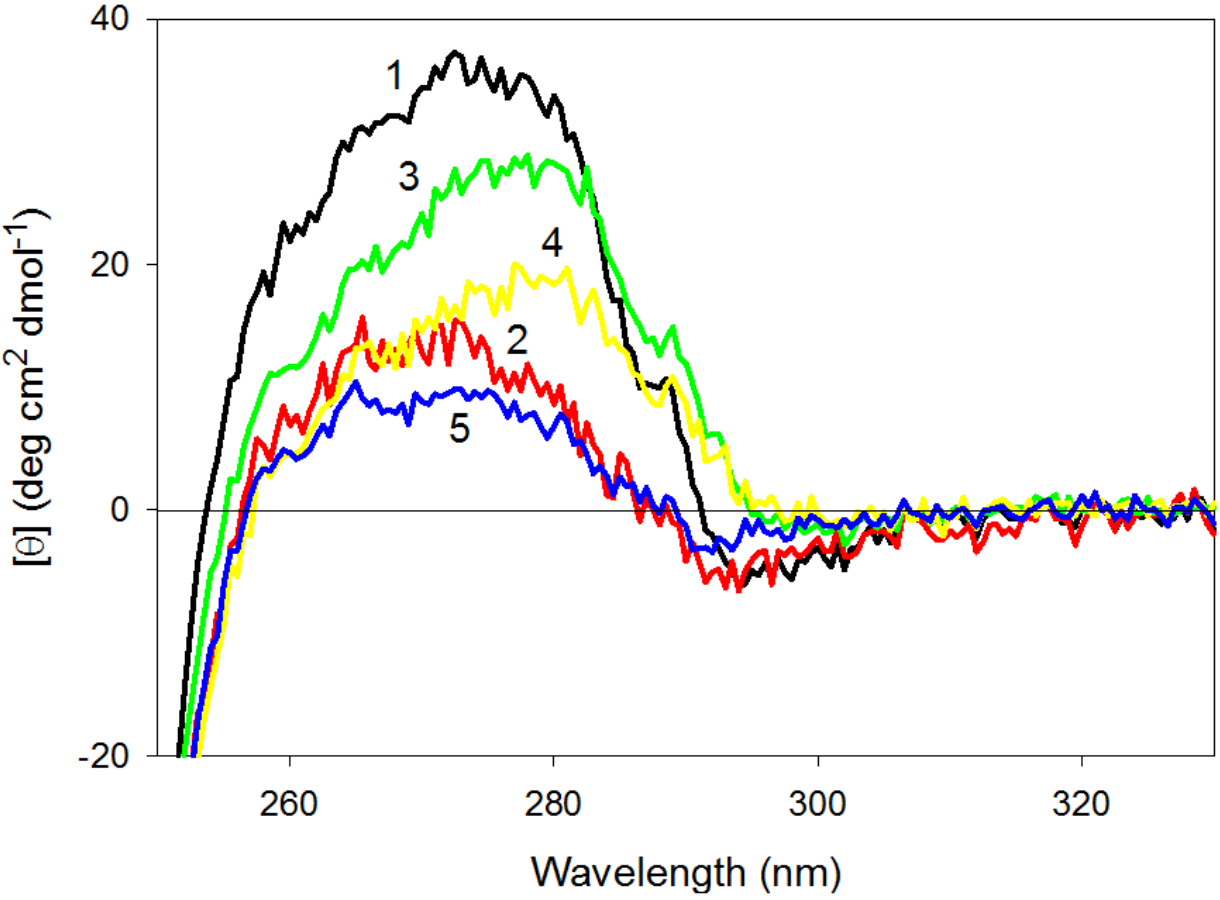

8

Near-UV CD spectra of the wild type (A), W674A (B), W707A (C), W737A (D) and W674A/W707A (E) CaD_{136} measured at different temperatures.

Figure 8. Near-UV CD spectra of the wild type (**A**), W674A (**B**), W707A (**C**), W737A (**D**) and W674A/W707A (**E**) CaD_{136} measured at different temperatures: 15°C (**1**); 40°C (**2**), 90°C (**3**) and 15°C after the cooling (**4**). All measurements were carried out at a protein concentration of 0.6-0.8 mg/ml, cell pathlength 10 mm.

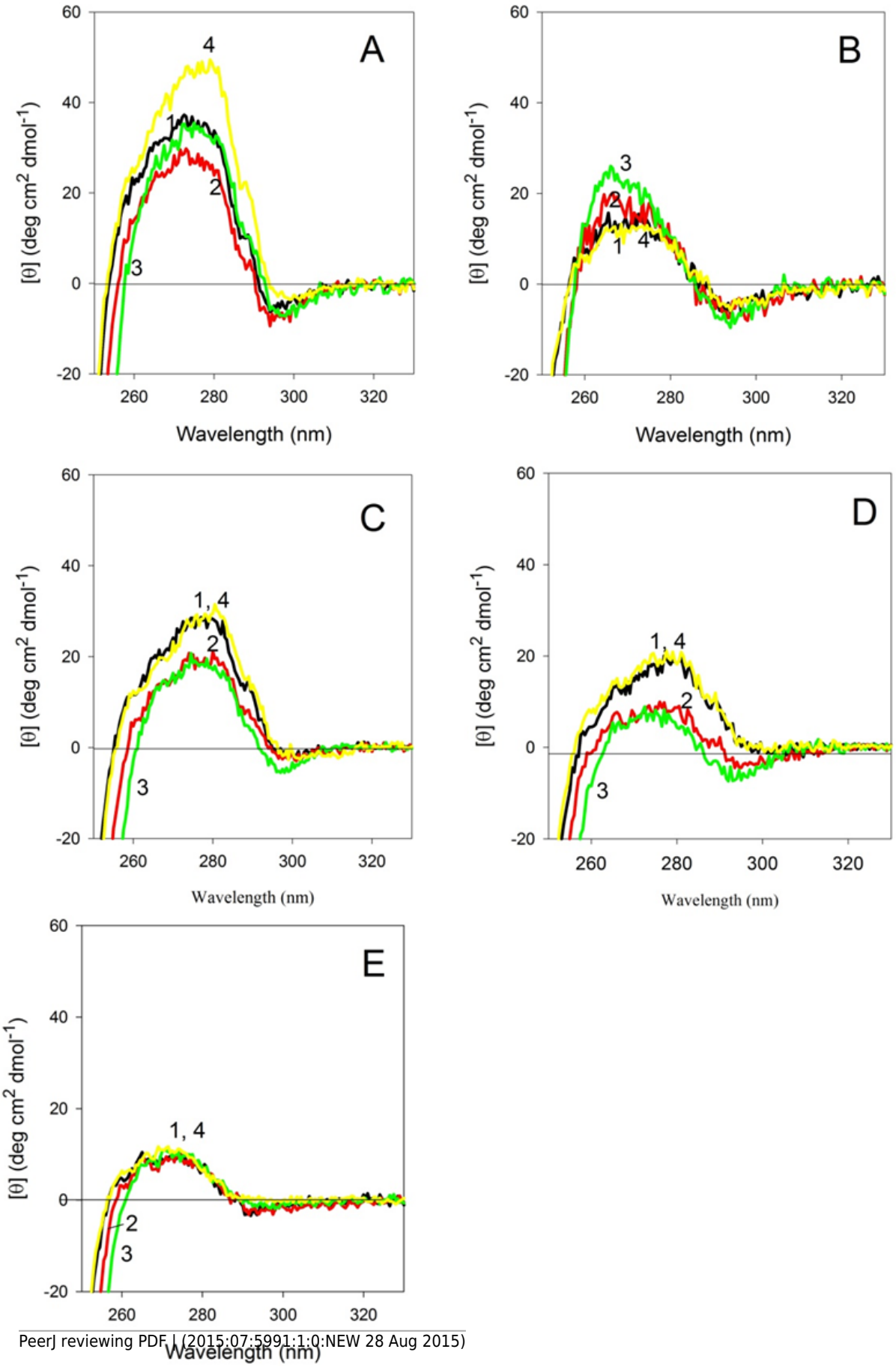
A
B
C
D
E
[θ] (deg cm2 dmol-1)
Wavelength (nm)
60
40
20
0
-20
260
280
300
320
1
2
3
4
1, 4

9

Effect of temperature on far-UV CD spectra of $CaD_{136.}$

Figure 9. A. Far-UV CD spectra of W674A mutant of CaD_{136} measured at different temperatures: 15°C (**1**); 40°C (**2**), 90°C (**3**) and 15°C after the cooling (**4**). All measurements were carried out at a protein concentration of 0.8 mg/ml, cell pathlength 0.1 mm. **B.** Effect of temperature on far-UV CD spectra of CaD_{136} and its mutants: wild type (**1**), W674A (**2**), W707A (**3**), W737A (**4**) and W674A/W707A (**5**).

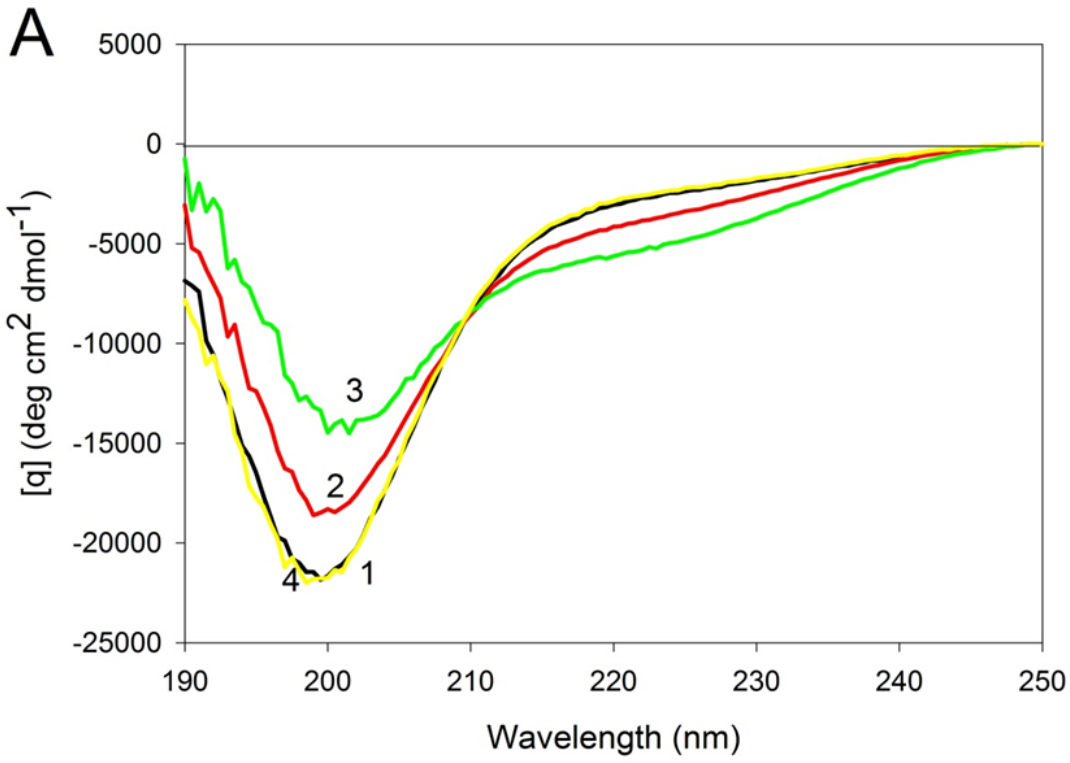
A
5000
0
-5000
-10000
-15000
-20000
-25000
[q] (deg cm2 dmol-1)
190
200
210
220
230
240
250
Wavelength (nm)
1
2
3
4

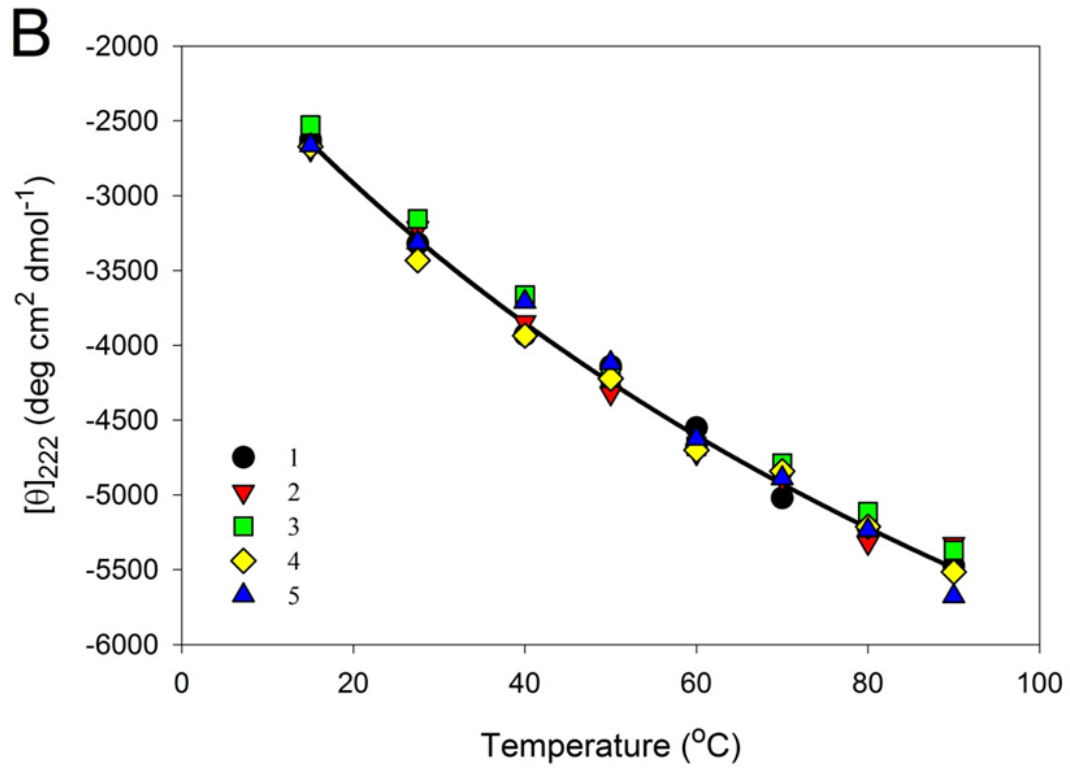
B
-2000
-2500
-3000
-3500
-4000
-4500
-5000
-5500
-6000
[θ]222 (deg cm2 dmol-1)
0
20
40
60
80
100
Temperature (°C)
1
2
3
4
5

10

Spectrofluorimetric titration of the CaD_{136} and its mutants by CaM.

Figure 10. Spectrofluorimetric titration of the CaD_{136} and its mutants by CaM.

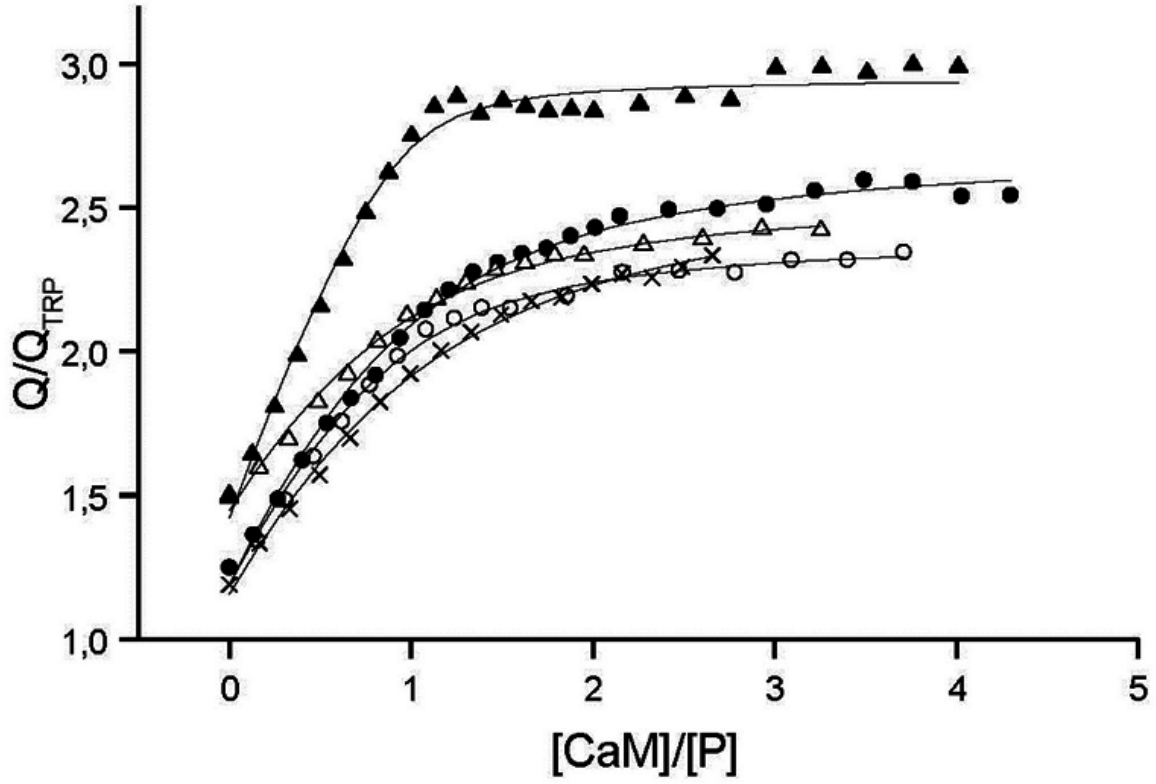
3,0
2,5
2,0
1,5
1,0
Q/Q_TRP
0
1
2
3
4
5
[CaM]/[P]

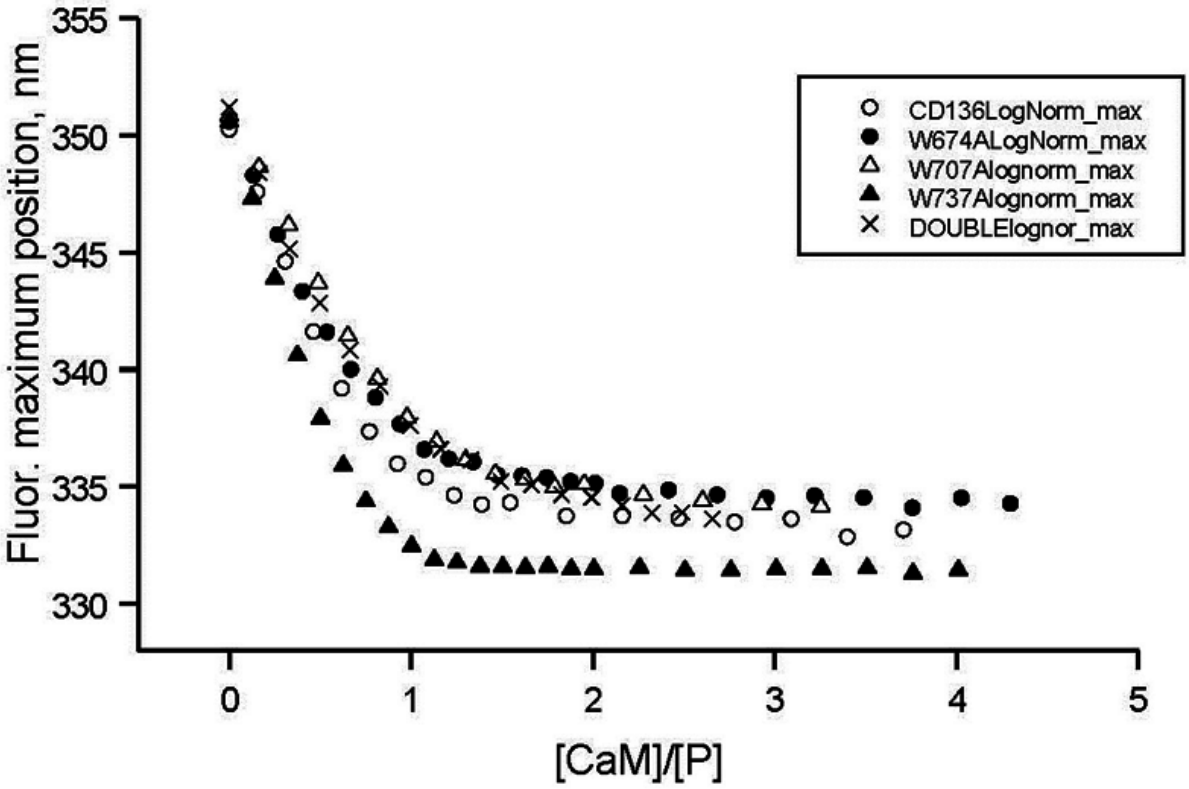
355
350
345
340
335
330
Fluor. maximum position, nm
CD136LogNorm_max
W674ALogNorm_max
W707Alognorm_max
W737Alognorm_max
DOUBLElognor_max
0
1
2
3
4
5
[CaM]/[P]

11

Schematic representation of the “buttons on a charge string” binding mode.

Figure 11. Schematic representation of the “buttons on a charge string” binding mode proposed in this study. Here, the CaD_{136} is shown as a blue string containing three “buttons” (tryptophan-centric partially structured binding sites), whereas CaM is shown as mostly red surface. Note that positions of binding sites and length of the CaD_{136} chain are arbitrary and used here only to illustrate an idea.